Synthesis, biological activity evaluation and molecular docking studies of novel thiazole derivatives

Derya Osmaniye[1,2], Uğur Kayış[3], Ülküye Dudu Gül[3], Yusuf Özkay[1,2],
Zafer Asım Kaplancıklı[✉1]

[1]Anadolu University, Faculty of Pharmacy, Department of Pharmaceutical Chemistry, Eskişehir, Türkiye.

[2]Anadolu University, Faculty of Pharmacy, Central Analysis Laboratory, Eskişehir, Türkiye.

[3]Bilecik Şeyh Edebali University, Biotechnology Application and Research Center, Vocational School of Health Services, Bilecik, Türkiye.

✉ Zafer Asım Kaplancıklı
    zakaplan@anadolu.edu.tr

ABSTRACT

Resistance to existing drugs develops because of insensible use of antibacterial and antifungal drugs. Therefore, there is a need for the development of new drug candidate compounds. The thiazole ring has many biological activities. It is possible to include antibacterial and antifungal activities among these activities. In addition to these, the thiazole ring has been preferred because it is the bioisostere of the imidazole ring in the structure of many antifungal drugs. For this purpose, within the scope of this study, 7 new thiazole compounds were synthesized, and their structure determinations were carried out using HRMS, ^{1}H-NMR, ^{13}C-NMR spectroscopic methods. Their antibacterial and antifungal activities were investigated by *in vitro* methods. As a result of activity tests, compound **3e** showed activity against *C.krusei* strain with $MIC_{50}=31.25$ ug/mL. The potential effectiveness of the compound **3e** on the 14alpha-demethylase enzyme (PDB ID:3LD6) was tested by *in silico* studies.

Keywords: Thiazole, Antibacterial Activity, Antifungal Activity, Molecular Docking

1. INTRODUCTION

Bacterial pathogen infections, which have become quite common in recent years, pose a danger to public health [1]. Causing some pathogens to escape the existing arsenal of antibiotics, causing health emergencies and major socio-economic impacts; The abuse or misuse of antibiotics in humans, animals, and agricultural practices perpetuates the need for new drug candidate molecules [2].

Nitrogen-containing heterocyclic analogs are of great interest in drug discovery. This is due to the well-known activities of these analogues in the pharmaceutical and medical fields [3]. Many heterocyclic compounds bearing a five-membered ring are known to be rich in

biological activity. Thiazole was first reported as an effective nucleus by Hantzsch and Weber in 1887. This ring system has also attracted intense interest from industrial and pharmaceutical researchers in recent years [4]. In addition to this information, Nitrogen-based heterocycles (especially those bound to phenolic substrates) are popular for their pharmacological properties, including their anticancer, anti-malarial, antitubercular, and antimicrobial activities [5]. In the literature studies on the thiazole ring, studies on the antibacterial and antifungal activities of this ring are frequently presented [6-15]. In addition to these, the thiazole ring has been preferred because it is the bioisostere of the imidazole ring in the structure of many antifungal drugs.

The imidazole ring system is present in many antifungal drugs (miconazole, ketoconazole). This group of drugs, called azoles, constitutes a group of drugs in antifungal therapy. It was thought that an imidazole ring-like effect could be created by using the thiazole ring. At the same time, there are examples where drugs containing the azole group have an antibacterial effect (metronidazole). New derivatives showing both effects are important in this field.

In this study, 7 new compounds containing thiazole ring were synthesized, their structures were determined, and their antibacterial and antifungal effects were investigated. In addition to the thiazole ring, the piperazine ring, which is also in the structure of many antifungal agents, is also included in the structure.

2. MATERIALS AND METHODS

2.1. Chemistry

The description of the synthesis pathways of the compounds is given below. The synthesized compounds were subjected to spectral analysis for structure determination. NMR spectra (^{1}H-NMR and ^{13}C-NMR) were performed using Bruker DPX 300 FT-NMR spectrometer and Bruker DPX 75 MHz spectrometer, respectively. LCMS-IT-TOF (Shimadzu, Kyoto, Japan) device was used for high resolution Mass spectra (HRMS). Electron spray ionization (ESI) was used as the ionization technique. While the numerical data of the obtained results are presented in **Table-1**; spectra are presented in the Supporting Information file (**Figure S1-S21**).

2.1.1. Synthesis of 4-(4-acetylpiperazin-1-yl) benzaldehyde (1).

1-(Piperazin-1-yl)ethan-1-one (0.039 mol, 5 gr) and 4-fluorobenzaldehyde (0.039 mol, 4.836 gr) were dissolved in DMF (dimethylformamide) in presence of potassium carbonate. And reaction mixture was refluxed for 36h. At the end of the reaction, the product, which was cooled and poured into ice water, solidified. The solid product was filtered off, washed 3 times with water and dried.

2.1.2. Synthesis of 2-(4-(4-acetylpiperazin-1-yl) benzylidene)hydrazine-1-carbothioamide (2)

Compound **1** (0.017 mol, 3.944 gr) was dissolved in absolute ethanol. Thiosemicarbazide (0.017 mol, 1.547 gr) was added in reaction mixture and this mixture was refluxed for 12 h. The end of the reaction was checked with TLC, the product precipitated solidly in the reaction medium. This precipitate was filtered off and dried by washing with cold ethanol.

2.1.3. Synthesis of target compounds (3a-3h)

Compound **2** (0.001 mol, 0.305 gr) and suitable phenylacylbromidederivatives (0.001 mol) were refluxed in absolute ethanol for 12h. The end of the reaction was checked with TLC, the product precipitated solidly in the reaction medium. This precipitate was filtered off, dried and crystallized from hexane.

2.2. Antibacterial and anticandidal activity

The activity study of synthesized compounds (**3a-3g**) was evaluated on eight bacterial and three fungal strains according to the standart procedure of CLSI [16] as designated in the prior study [17]. The strains used for both antibacterial and antifungal activity are listed in Table-2. ATCC codes are as follows; ATCC 6051, ATCC 25922, ATCC 2942, ATCC 13883, ATCC 27853, ATCC 29213, ATCC 12228, ATCC 8100. ATCC 6258, ATCC 24433, ATCC 22019.

2.3. Prediction of ADME Parameters

SwissADME (online) were used for prediction of ADME parameters [18].

2.4. Molecular Docking Study

Molecular docking studies were performed using *in-silico* procedure to define the binding modes of compound **3e** (NO_2 containing compound) in the active regions of enzymes X-ray crystal structures of 14alpha-demethylase (PDB ID:3LD6) [19] were retrieved from Protein Data Bank server (www.pdb.org, accessed 25.02.2022). Molecular docking studies were performed as previously reported [20-22].

Table 1. Spectral analysis results of compounds **3a-3g**

Compounds	¹H-NMR	¹³C-NMR	HRMS
3a	2.04 (3H, s, -COCH$_3$), 3.22 (2H, br.s., piperazine), 3.28 (2H, br.s., piperazine), 3.58 (4H, br.s., piperazine), 7.04 (2H, d, *J*=8.4 Hz, Ar-H), 7.29-7.33 (2H, m, Ar-H), 7.41 (2H, t, *J*=7.3 Hz, Ar-H), 7.54 (2H, d, *J*=8.5 Hz, Ar-H), 7.84 (2H, d, *J*=8.5 Hz, Ar-H), 7.99 (1H, s, Ar-H).	21.65, 45.55, 48.15, 48.49, 103.87, 115.93, 125.68, 126.08, 128.09, 128.19, 129.10, 134.52, 142.99, 149.78, 151.32, 168.79, 168.82	calcd for C$_{22}$H$_{23}$N$_5$OS: 406.1696; found 406.1686.
3b	2.05 (3H, s, -COCH$_3$), 2.32 (3H, s, -CH$_3$), 3.18-3.22 (2H, m, piperazine), 3.25-3.28 (2H, m, piperazine), 3.58 (4H, br.s., piperazine), 7.00 (2H, d, *J*=8.8 Hz, Ar-H), 7.20-7.22 (3H, m, Ar-H), 7.53 (2H, d, *J*=8.8 Hz, Ar-H), 7.74 (2H, d, *J*=8.1 Hz, Ar-H), 7.94 (1H, s, Ar-H).	21.27, 21.66, 45.67, 47.85, 48.21, 102.74, 115.63, 125.34, 125.93, 127.91, 129.63, 132.44, 137.24, 142.24, 150.72, 151.70, 168.71, 168.79	calcd for C$_{23}$H$_{25}$N$_5$OS: 420.1853; found 420.1860.
3c	2.05 (3H, s, -COCH$_3$), 3.18-3.21 (2H, m, piperazine), 3.25-3.28 (2H, m, piperazine), 3.56-3.58 (4H, m, piperazine), 3.78 (3H, s, -OCH$_3$), 6.95-7.01 (4H, m, Ar-H), 7.10 (1H, s, Ar-H), 7.51 (2H, d, *J*=8.8 Hz, Ar-H), 7.78 (2H, d, *J*=8.8 Hz, Ar-H), 7.92 (1H, s, Ar-H), 11.90 (1H, s, -NH).	21.70, 40.93, 45.70, 47.83, 48.18, 55.60, 101.52, 114.39, 115.59, 125.34, 127.27, 127.86, 128.12, 141.97, 151.75, 159.18, 159.19, 168.69, 168.78.	calcd for C$_{23}$H$_{25}$N$_5$O$_2$S: 436.1802; found 436.1818
3d	2.05 (3H, s, -COCH$_3$), 3.19-3.22 (2H, m, piperazine), 3.25-3.29 (2H, m, piperazine), 3.56-3.58 (4H, m, piperazine), 7.01 (2H, d, *J*=8.9 Hz, Ar-H), 7.52 (2H, d, *J*=8.9 Hz, Ar-H), 7.61 (1H, s, Ar-H), 7.87 (2H, d, *J*=8.7 Hz, Ar-H), 7.96 (1H, s, Ar-H), 8.03 (2H, d, *J*=8.5 Hz, Ar-H), 12.02 (1H, s, -NH).	21.70, 45.69, 47.77, 48.13, 107.59, 109.95, 115.54, 119.49, 125.12, 126.55, 127.98, 133.15, 139.32, 142.62, 149.28, 151.84, 168.77, 169.12	calcd for C$_{23}$H$_{22}$N$_6$OS: 431.1649; found 431.1651
3e	2.05 (3H, s, -COCH$_3$), 3.21-3.22 (2H, m, piperazine), 3.27-3.29 (2H, m, piperazine), 3.58 (4H, br.s., piperazine), 7.01 (2H, d, *J*=8.9 Hz, Ar-H), 7.53 (2H, d, *J*=8.8 Hz, Ar-H), 7.68 (1H, s, Ar-H), 7.96 (1H, s, Ar-H), 8.11 (2H, d, *J*=8.9 Hz, Ar-H), 8.26-8.29 (2H, m, Ar-H), 12.07 (1H, s, -NH).	21.65, 40.93, 45.68, 47.76, 48.11, 108.58, 115.53, 124.57, 125.08, 126.76, 127.99, 141.22, 142.74, 146.60, 148.97, 151.86, 168.78, 169.22	calcd for C$_{22}$H$_{22}$N$_6$O$_3$S: 389.1152; found 389.1134
3f	2.05 (3H, s, -COCH$_3$), 3.18-3.21 (2H, m, piperazine), 3.24-3.28 (2H, m, piperazine), 3.57-3.59 (4H, m, piperazine), 6.99 (2H, d, *J*=8.9 Hz, Ar-H), 7.36 (1H, s, Ar-H), 7.46 (2H, d, *J*=8.6 Hz, Ar-H), 7.53 (2H, d, *J*=8.8 Hz, Ar-H), 7.87 (2H, d, *J*=8.6 Hz, Ar-H), 7.95 (1H, s, Ar-H), 11.97 (1H, s, -NH).	21.66, 40.92, 45.68, 47.79, 48.14, 104.47, 115.56, 125.22, 127.66, 127.92, 129.07, 132.30, 134.09, 142.31, 149.71, 151.79, 168.77, 168.95	calcd for C$_{22}$H$_{22}$N$_5$OSCl: 440.1306; found 440.1299
3g	2.05 (3H, s, -COCH$_3$), 3.18-3.21 (2H, m, piperazine), 3.25-3.28 (2H, m, piperazine), 3.57-3.58 (4H, m, piperazine), 6.99 (2H, d, *J*=8.9 Hz, Ar-H), 7.36 (1H, s, Ar-H), 7.52 (2H, d, *J*=8.9 Hz, Ar-H), 7.60 (2H, d, *J*=8.6 Hz, Ar-H), 7.81 (2H, d, *J*=8.6 Hz, Ar-H), 7.94 (1H, s, Ar-H), 11.97 (1H, s, -NH).	21.67, 40.93, 45.68, 47.79, 48.14, 104.56, 115.56, 120.89, 125.21, 127.93, 127.97, 131.98, 134.43, 142.31, 149.78, 151.80, 168.77, 168.94	calcd for C$_{22}$H$_{22}$N$_5$OSBr: 484.0801; found 484.0814

Table 2. Antibacterial and anticandidal activity of synthesized compounds (**3a-3g**) and standart drugs (**SD1-SD3**)

ID	Antibacterial activity MIC$_{50}$ (μg/mL) [a]								Anticandidal activity MIC$_{50}$ (μg/mL) [b]		
	B.subtilis	E.coli	E.faecalis	K.pneumoniae	P.aeruginosa	S.aureus	S.epidermis	S.marcescens	C. albicans	C. krusei	C. parapsilopsis
3a	125	125	125	125	62.5	62.5	125	62.5	62.5	62.5	62.5
3b	125	62.5	125	125	62.5	62.5	125	62.5	62.5	62.5	62.5
3c	125	62.5	125	125	62.5	62.5	125	62.5	125	62.5	62.5
3d	125	125	125	125	62.5	125	125	62.5	125	62.5	62.5
3e	125	125	125	62.5	62.5	62.5	125	62.5	62.5	31.25	62.5
3f	125	125	125	125	125	125	125	62.5	125	62.5	62.5
3g	125	125	125	125	125	125	125	62.5	125	62.5	62.5
SD1	< 0.97	< 0.97	< 0.97	< 0.97	< 0.97	< 0.97	< 0.97	< 0.97	-	-	-
SD2	-	-	-	-	-	-	-	-	3.90	3.90	1.95
SD3	-	-	-	-	-	-	-	-	7.81	7.81	3.90

[a] The test results were expressed as means of triplicate assays. [b] The test results were expressed as means of triplicate assays. [c] The test results were expressed as means of quartet assays ± SEM. SD1: Azithromycin. SD2: Voriconazole. SD3: Fluconazole

Compounds	R
3a	-H
3b	-CH₃
3c	-OCH₃
3d	-CN
3e	-NO₂
3f	-Cl
3g	-Br
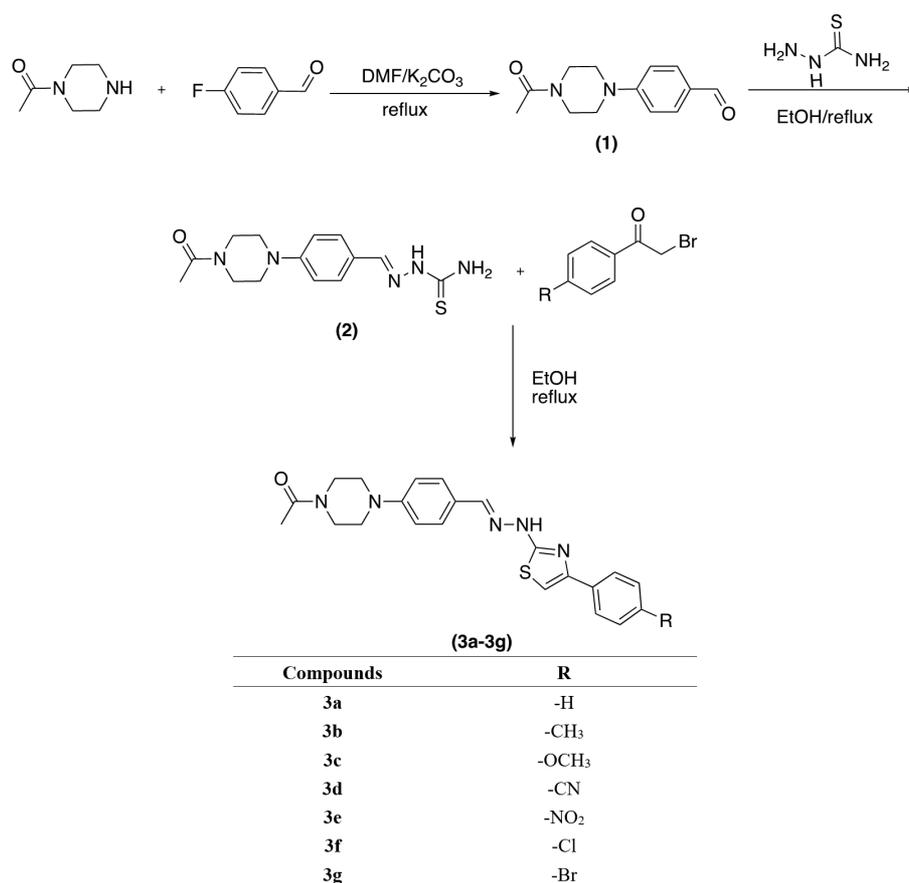
Scheme 1. Synthesis pathway for obtained compounds **(3a-3g)**

3. RESULTS AND DISCUSSION

3.1. Chemistry

The compounds **3a-3g** were obtained as presented in **Scheme 1**. Initially, aldehyde derivative (**1**) was obtained by means of the reaction between 1-(piperazin-1-yl)ethan-1-one and 4-fluorobenzaldehyde using potassium carbonate. Secondly, the thiosemicarbazone derivative (**2**) was obtained by means of reaction between 4-(4-acetylpiperazin-1-yl)benzaldehyde and thiosemicarbazide. The target compounds (**3a-3g**) were obtained using ring closure reaction. The structures of the compounds **3a-3g** were evaluated by using spectroscopic methods (HRMS, ¹H-NMR and ¹³C-NMR).

When the NMR data of the compounds are examined, it is seen that the protons of piperazine come in the form of 2H, 2H, 4H, between 3.18 ppm and 3.59 ppm. Protons of the acetyl group attached to piperazine were recorded as singlet between 2.04 ppm and 2.05 ppm. The carbon belonging to this group was recorded between 21.27 ppm and 21.70 ppm values. In addition, the carbonyl carbon of this group was recorded between 168.78 ppm and 169.22 ppm. While the methyl group of compound **3b** was recorded as a singlet at 2.32 ppm; The methoxy group of compound **3c** was recorded as singlet at 3.78 ppm. Mass spectra were performed using high resolution liquid chromatography. In the mass spectra taken using the electron spray method, all compounds were recorded as an excess of their molecular weights.

3.2. Antibacterial and anticandidal activity

Eight bacterial strains (it can be seen in **Table-2**) were used to evaluate the antibacterial activity of the obtained compounds (**3a-3g**). Azithromycin was used as the reference drug in fluorometric measurements of which MIC_{50} values were calculated using resazurin solution [23-24]. The results are presented in **Table 2**. When **Table-2** is examined, it is seen that the antibacterial MIC_{50} values of the compounds **3a-3g** were determined between 62.5-125 ug/mL.

Three candida strains (it can be seen in **Table-2**) were used to evaluate the antifungal activity of the obtained compounds (**3a-3g**). Voriconazole and fluconazole were used as the reference drug in fluorometric measurements of which MIC_{50} values were calculated using resazurin solution [23,24]. The results are presented in **Table 2**. When **Table-2** is examined, it is seen that the antifungal MIC_{50} values of the compounds **3a-3g** were determined between 31.25-125 ug/mL. Compound **3e** was the most active compound with MIC_{50}=31.25 ug/mL against *C. krusei*. However, this activity value is not as high as predicted. When the structure of the compound is examined, the nitro group in its structure is remarkable compared to other compounds. The nitro group contributed a little to the activity. However, in general, MIC_{50} values in the series suggest that one or more of the common structures negatively affect the activity. For this purpose, *in silico* molecular docking studies of the compounds were carried out.

It is known that azole group compounds exert their antifungal activities by inhibiting ergosterol biosynthesis. They inhibit the conversion of lanosterol molecule to ergosterol by inhibition of 14alpha-demethylase enzyme. The antifungal activity of compound **3e** on *C.krusei* is promising. However, modifications can be made to the molecule to increase this efficiency. For this reason, first, how the compound acts in the active site of the enzyme should be examined. *In silico* studies were carried out using compound **3e** and 14alpha-demethylase enzyme crystal for this purpose.

3.3. Prediction of ADME Parameters

The physicochemical properties of drugs provide important information about their ability to be a drug. Thanks to these parameters that can be calculated online, an impression is gained about the drug profile of the compounds. The online SwissADME program was used and the estimated ADME parameters of the obtained compounds were calculated [18]. When **Table-3**, in which the results are presented, is examined, it is seen that none of the compounds with positive drug candidate potential violate the Lipinski rule [25]. It is also a positive feature that the Lipinski rule violation values are zero. Gastrointestinal absorption is an important parameter for oral administration of compounds. When the pharmacokinetic part is examined, the high gastrointestinal absorption profiles of all

Table 3. Predicted ADME parameters of compounds **3a-3g**

| Comp	Physicochemical Properties						Pharmaco-kinetics			Drug likeness		Medicinal Chemistry
	HBA	HBD	TPSA	Log Po/w	LogS	GIA	Log Kp	BBB permeant	P-gp substrate	Lipinski	Vio	SA
3a	3	1	89.07	3.10	-4.89	High	-5.96	No	No	Yes	0	3.47
3b	3	1	89.07	3.32	-5.19	High	-5.79	No	No	Yes	0	3.59
3c	4	1	98.30	3.38	-4.96	High	-6.17	No	No	Yes	0	3.54
3d	4	1	112.86	3.09	-4.84	High	-6.31	No	No	Yes	0	3.58
3e	5	1	134.89	2.52	-4.95	High	-6.36	No	No	Yes	0	3.60
3f	3	1	89.07	3.46	-5.48	High	-5.72	No	No	Yes	0	3.46
3g	3	1	89.07	3.56	-5.80	High	-5.95	No	No	Yes	0	3.50
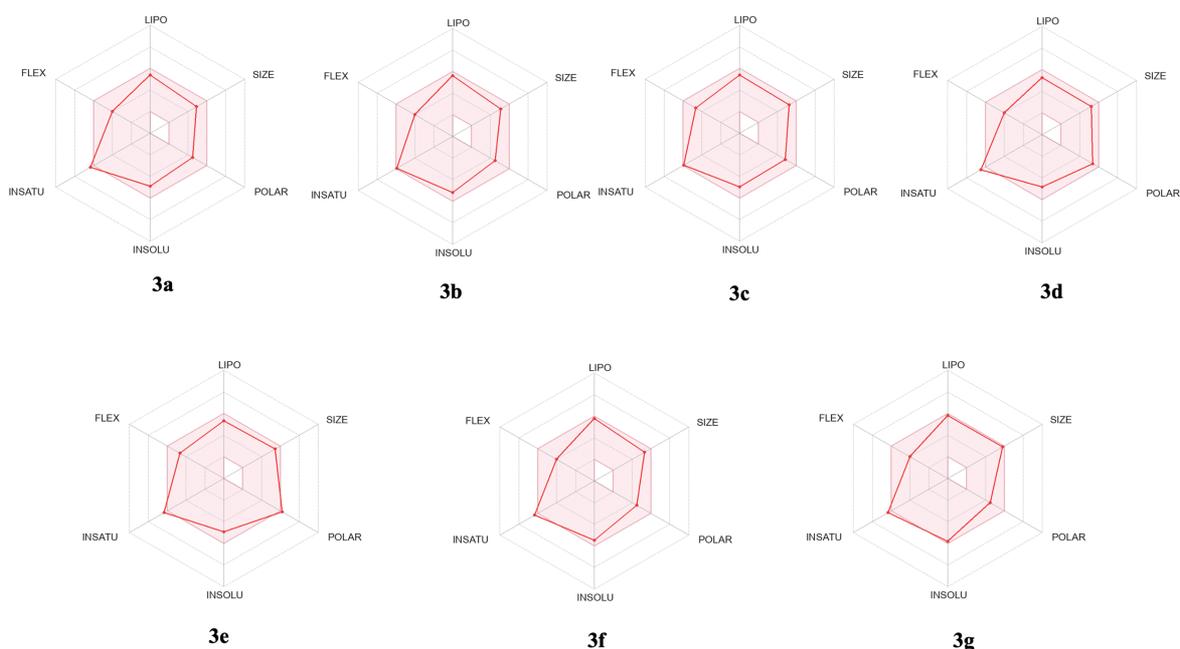
Figure 1. Oral bioavailability radars of obtained compounds **(3a-3g)**

compounds indicate the oral use potential of the compounds. The hydrophilic-lipophilic properties diagram of the compound **3e** were presented using the Molinsparition program (**Figure 1**). The synthetic accessibility (SA) value gets harder from 1 to 10 [26]. This value is an important value for synthetic chemistry. There is no compound approaching or exceeding 10 in compound **3a-3g**. The SA values of the compounds ranged between 3.47 and 3.60. P-gp causes excretion of some drugs, so the pharmacokinetic efficacy is reduced. It is also known that some cancer cells cause an increase in the amount of this protein and cause drug resistance because of drugs acting as P-gb substrate. Examining **Table-3**, none of the compounds (**3a-3g**) act as a substrate for P-gp. As a result, it is seen that all compounds have suitable physicochemical parameters. This demonstrates the value of compounds. Especially the high gastrointestinal permeability will allow the oral use of the compounds.

3.3. Molecular Docking Studies

To elucidate the antifungal action mechanism of compound **3e**, which is the most active derivative according to the activity result, it was subjected to *in silico* insertion procedure with 14alpha-demethylase

(PDB ID:3LD6). The placement of the compound in the enzyme active site is shown in **Figure-2**. Compound **3e** appears to localize to the enzyme active site. The thiazole ring of the compound is located close to the HEM molecule in the enzyme active site. This may be a suitable placement for the azole group.

Docking studies were performed on the 14alpha-demethylase crystals (PDB ID:3LD6) [19] for approved binding model. **Figure-3** shows the 3D localization of compound **3e** in the enzyme active site. The bonds formed by compound **3e** at the enzyme active site can be summarized as follows. A hydrogen bond is formed between the nitro group of compound **3e** and the amino group of Ile488. Aromatic hydrogen bonds are formed between the phenyl ring of the 4-nitrophenyl group and the carbonyl group of Met487 and Pro376. Pi-pi interaction was established between the thiazole ring of compound **3e** and phenyl ring of Phe234.

In addition to these interactions, compound **3e** does not interact with the HEM group in the enzyme active site. This lack of interaction may be the reason for the low activity value compared to the reference drugs.
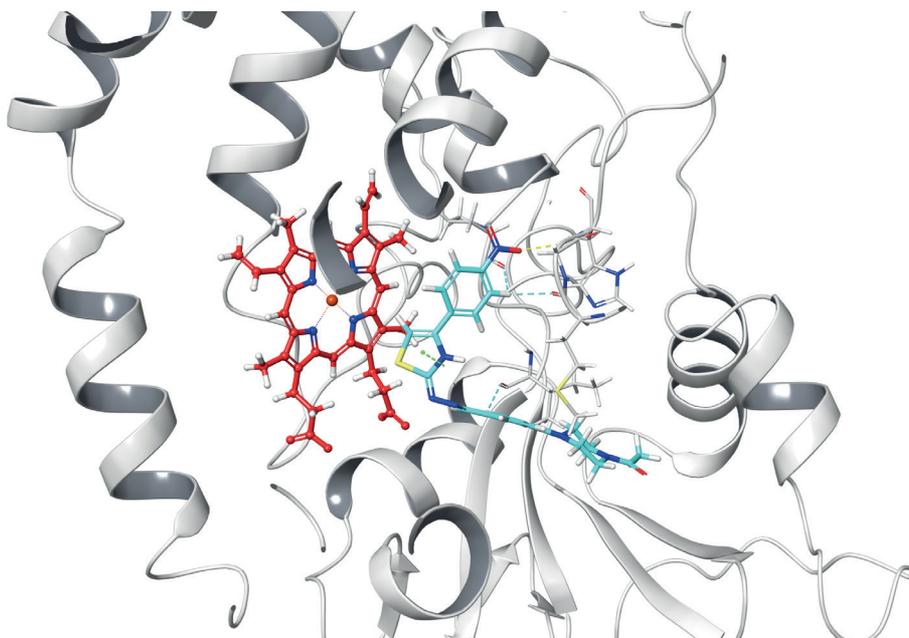
**Figure 2.** Localization of compound **3e** in the enzyme active site (PDB ID:3LD6)
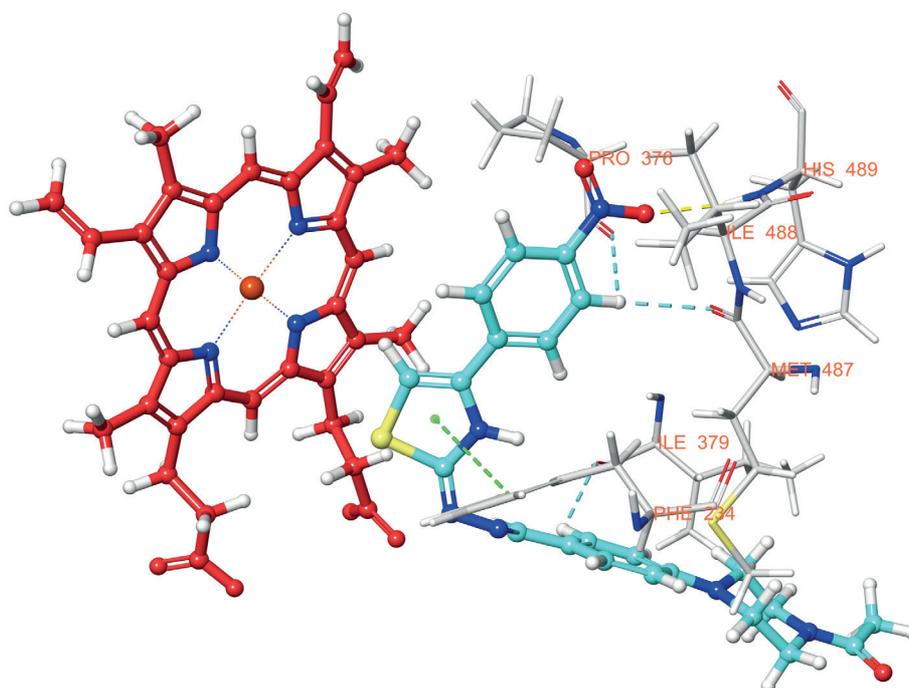
Figure 3. The three-dimensional interacting mode of compound **3e** in the active region of 14alpha-demethylase enzyme (PDB ID: 3LD6)

4. CONCLUSION

Frequent and uncontrolled use of antibiotics and antifungal drugs causes the development of resistance. Resistance to drugs with clinical use is a risk factor especially for patients in critical condition. For this reason, the need to develop new antibacterial and antifungal drugs always continues. It is known that azole group compounds constitute most antifungal drugs. These ring systems, which also have antibacterial activity, are molecules with an antimicrobial activity profile.

The strategy of designed new compounds using pharmacophore structures with proven activity are a frequently preferred method for medicinal chemists. The thiazole ring has a wide range of activity profile. Within the scope of this study, 7 compounds containing thiazole were synthesized, their structure determinations were carried out and their biological activities were determined by *in vitro* methods. Compound **3e** showed activity on the *C.krusei* line with a value of MIC_{50}=31.25 ug/ml. This activity value is 4 times lower than the reference drug fluconazole (MIC_{50}=7.81 ug/mL against *C.krusei*). No antibacterial activity was detected. While the compounds do not show antibacterial activity, they exhibit antifungal activity, suggesting that the mechanism of action may be based on the azole group. Molecular docking studies were carried out to better understand the reason for this difference and to determine the points to be considered in the design of new compounds. It is known that azole group compounds perform their antifungal activities by inhibiting ergosterol biosynthesis. The azole group antifungal agents inhibit the 14alpha-demethylase enzyme. Molecular docking studies due to the thiazole structure were carried out using 14alpha-demethylase crystal (PDB ID:3LD6). Here it is seen that the piperazine group of the compound **3e** does not contribute to the enzyme active site. The changing of more smaller volume groups can provide the compound's approximation to the HEM molecule. For this purpose, new compounds will be designed by keeping 4-nitrophenyl and thiazole structures constant based on this compound in future studies. And so, the activity is thought to increase.

REFERENCES

1. Yang XC, Zeng CM, Avula SR, Peng XM, Geng RX, Zhou CH. Novel coumarin aminophosphonates as potential multitargeting antibacterial agents against Staphylococcus aureus. Eur. J. Med. Chem. (2023); 245: 114891. https://doi.org/10.1016/j.ejmech.2022.114891

2. Zhou XM, Hu YY, Fang B, Zhou CH. Benzenesulfonyl thiazoloimines as unique multitargeting antibacterial agents towards Enterococcus faecalis. Eur. J. Med. Chem. (2023); 115088. https://doi.org/10.1016/j.ejmech.2023.115088

3. Rashdan HR, Abdelmonsef AH, Abou-Krisha MM, Yousef TA. Synthesis, identification, computer-aided docking studies, and ADMET prediction of novel benzimidazo-1, 2, 3-triazole based molecules as potential antimicrobial agents. Molecules (2021); 26(23): 7119. https://doi.org/10.3390/molecules26237119

4. Niu ZX, Wang YT, Zhang SN, Li Y, Chen XB, Wang SQ, Liu HM. Application and synthesis of thiazole ring in clinically approved drugs. Eur. J. Med. Chem (2023); 250: 115172. https://doi.org/10.1016/j.ejmech.2023.115172

5. Hussein AHM, El-Adasy ABA, El-Saghier AM, Olish M, Abdelmonsef AH. Synthesis, characterization, *in silico* molecular docking, and antibacterial activities of some new nitrogen-heterocyclic analogues based on ap-phenolic unit. RSC Adv. (2022); 12(20): 12607-12621. https://doi.org/10.1039%2Fd2ra01794f

6. Mokariya JA, Rajani DP, Patel MP. 1, 2, 4-Triazole and benzimidazole fused dihydropyrimidine derivatives: Design, green synthesis, antibacterial, antitubercular, and antimalarial activities. Arch. Pharm. (2022); e2200545. https://doi.org/10.1002/ardp.202200545

7. Nural Y, Ozdemir S, Yalcin MS, Demir B, Atabey H, Seferoglu Z, Ece A. New bis-and tetrakis-1, 2, 3-triazole derivatives: Synthesis, DNA cleavage, molecular docking, antimicrobial, antioxidant activity and acid dissociation constants. Bioorg. Med. Chem. Lett. (2022); 55: 128453. https://doi.org/10.1016/j.bmcl.2021.128453

8. Hu Y, Hu C, Pan G, Yu C, Ansari MF, Bheemanaboina RRY, Cheng Y, Chenghe Z, Zhang, J. Novel chalcone-conjugated, multi-flexible end-group coumarin thiazole hybrids as potential antibacterial repressors against methicillin-resistant Staphylococcus aureus. Eur. J. Med. Chem. (2021); 222: 113628. https://doi.org/10.1016/j.ejmech.2021.113628

9. Sucharitha ER, Krishna TM, Manchal R, Ramesh G, Narsimha S. Fused benzo [1, 3] thiazine-1, 2, 3-triazole hybrids: Microwave-assisted one-pot synthesis, *in vitro* antibacterial, antibiofilm, and *in silico* ADME-studies. Bioorg. Med. Chem. Lett. (2021); 47: 128201. https://doi.org/10.1016/j.bmcl.2021.128201

10. Gondru R, Kanugala S, Raj S, Kumar CG, Pasupuleti M, Banothu J, Bavantula R. 1, 2, 3-triazole-thiazole hybrids: Synthesis, *in vitro* antimicrobial activity and antibiofilm studies. Bioorg. Med. Chem. Lett. (2021); 33: 127746. https://doi.org/10.1016/j.bmcl.2020.127746

11. Salih RHH, Hasan AH, Hussen NH, Hawaiz FE, Hadda TB, Jamalis J, Almalki FA, Adeyinka AS, Coetzee LCC, Oyebamiji, AK. Thiazole-pyrazoline hybrids as potential antimicrobial agent: synthesis, biological evaluation, molecular docking, DFT studies and POM-analysis. J. Mol. Struct. (2023); 1282(10): 135191. https://doi.org/10.1016/j.molstruc.2023.135191

12. Alqurashi RM, Farghaly TA, Sabour R, Shaabana MR. Design, Synthesis, antimicrobial screening and molecular modeling of novel 6, 7 dimethylquinoxalin-2 (1H)-one and thiazole derivatives targeting DNA gyrase enzyme. Bioorg. Chem. (2023); 134: 106433. https://doi.org/10.1016/j.bioorg.2023.106433

13. Nandurkar Y, Shinde A, Bhoye MR, Jagadale S, Mhaske PC. Synthesis and biological screening of new 2-(5-Aryl-1-phenyl-1H-pyrazol-3-yl)-4-aryl thiazole derivatives as potential antimicrobial agents. ACS Omega (2023); 8(9):8743-8754. https://doi.org/10.1021/acsomega.2c08137

14. Meng F, Yan Z, Lu Y, Wang X. Design, synthesis, and antifungal activity of flavonoid derivatives containing thiazole moiety. Chem. Pap. (2022); 77:877-885. https://doi.org/10.1007/s11696-022-02522-4

15. Jagadeesan S, Karpagam S. Novel series of N-acyl substituted indole based piperazine, thiazole and tetrazoles as potential antibacterial, antifungal, antioxidant and cytotoxic agents, and their docking investigation as potential Mcl-1 inhibitors. J. Mol. Struct. (2023); 1271: 134013. https://doi.org/10.1016/j.molstruc.2022.134013

16. Wikler MA. Methods for dilution antimicrobial susceptibility tests for bacteria that growl aerobically: approved standard. Clsi (Nccls) (2006); 26: M7-A7.

17. Evren AE, Dawbaa S, Nuha D, Yavuz ŞA, Gül ÜD, Yurttaş L. Design and synthesis of new 4-methylthiazole derivatives: *In vitro* and *in silico* studies of antimicrobial activity. J. Mol. Struct. (2021); 1241: 130692. https://doi.org/10.1016/j.molstruc.2021.130692

18. Swiss Institute of Bioinformatics. SwissADME. Retrieved December 1 2022 from http://www.swissadme.ch/index.php#

19. Strushkevich N, Usanov SA, Park HW. Structural basis of human CYP51 inhibition by antifungal azoles. J. Mol. Biol. (2010); 397(4): 1067-1078. https://doi.org/10.1016/j.jmb.2010.01.075

20. Maestro, *Schrödinger, LLC: New York, NY, USA* 2020.

21. Schrödinger, *Schrödinger, LLC, New York, NY, USA* 2020.

22. Schrödinger, *Schrödinger, LLC: New York, NY, USA* 2020.

23. Borra RC, Lotufo MA, Gagioti SM, Barros FDM, Andrade PM. A simple method to measure cell viability in proliferation and cytotoxicity assays. Braz. Oral. Res. (2009); 23: 255-262. https://doi.org/10.1590/S1806-83242009000300006

24. Palomino JC, Martin A, Camacho M, Guerra H, Swings J, Portaels F. Resazurin microtiter assay plate: simple and inexpensive method for detection of drug resistance in Mycobacterium tuberculosis. AMACCQ (2022); 46(8): 2720-2722. https://doi.org/10.1128/AAC.46.8.2720-2722.2002

25. Lipinski CA, Lombardo F, Dominy BW, Feeney PJ. Experimental and computational approaches to estimate solubility and permeability in drug discovery and development settings. Adv. Drug Deliv. Rev. (2012); 64: 4-17. https://doi.org/10.1016/S0169-409X(00)00129-0

26. Daina A, Michielin O, Zoete V. SwissADME: a free web tool to evaluate pharmacokinetics, drug-likeness and medicinal chemistry friendliness of small molecules. Sci. Rep. (2017); 7(1): 42717.

Supporting Information
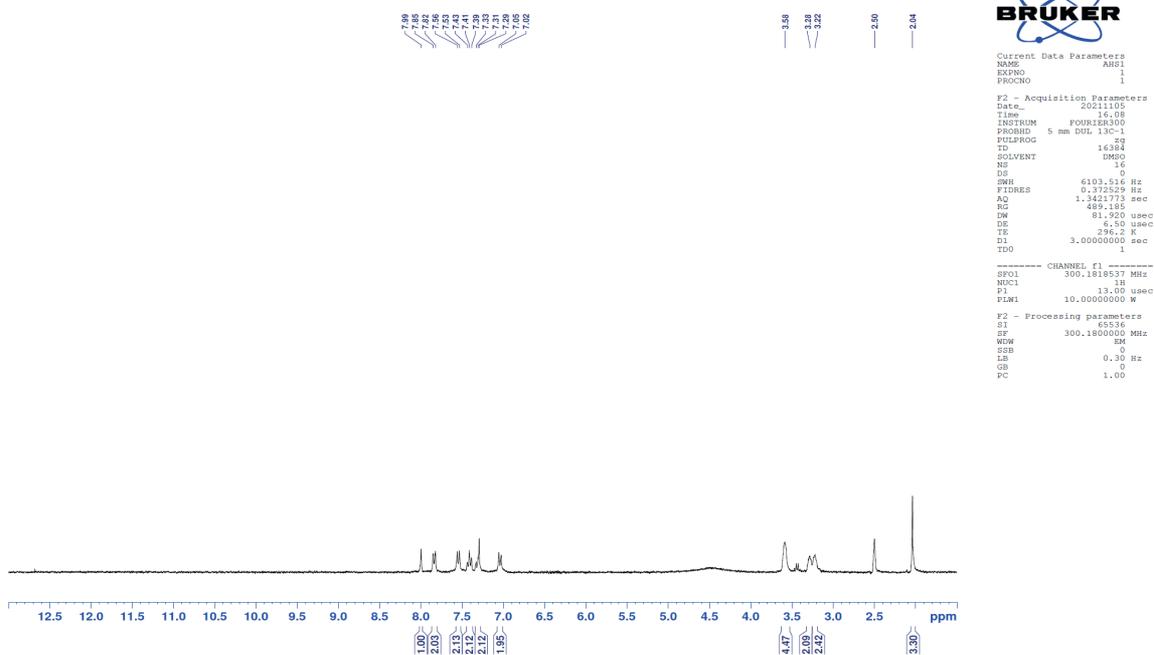

Figure S1. Compound **3a** ¹H-NMR spectrum
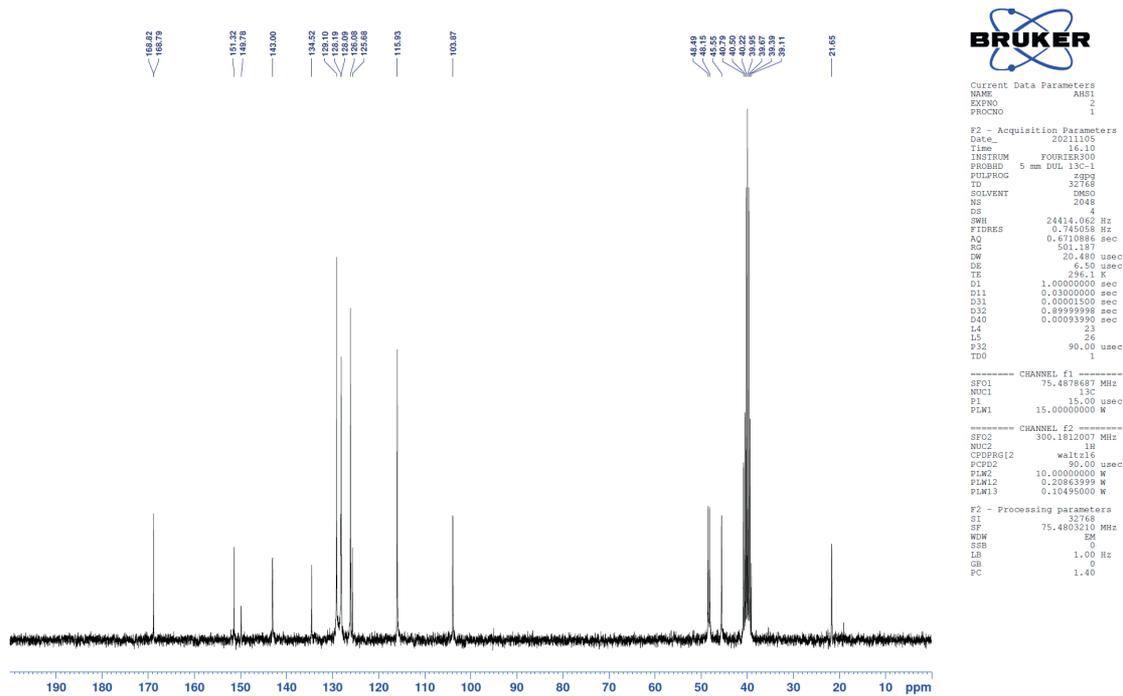
Figure S2. Compound **3a** ¹³C-NMR spectrum

Formula Predictor Report - AHS-1_111.lcd

Data File: C:\LabSolutions\Data\Analiz\derya\AHS-1_111.lcd

Elmt	Val.	Min	Max	Elmt	Val.	Min	Max	Elmt	Val.	Min	Max	Elmt	Val.	Min	Max	Use Adduct
H	1	6	46	O	2	0	3	S	2	0	2	Ru	2	0	0	H
C	4	5	36	F	1	0	0	Cl	1	0	0	Pd	2	0	0	
N	3	0	6	P	3	0	0	Br	1	0	0	I	3	0	0	

Error Margin (ppm): 5
HC Ratio: unlimited
Max Isotopes: 3
MSn Iso RI (%): 10.00

DBE Range: 0.0 - 30.0
Apply N Rule: yes
Isotope RI (%): 1.00
MSn Logic Mode: AND

Electron Ions: both
Use MSn Info: yes
Isotope Res: 9000
Max Results: 50

Event#: 1 MS(E+) Ret. Time : 4.573 -> 4.573 Scan# : 687 -> 687
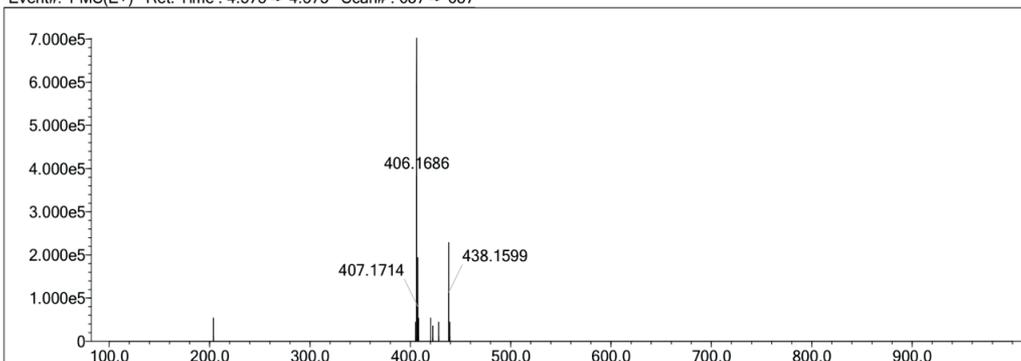
Measured region for 406.1686 m/z
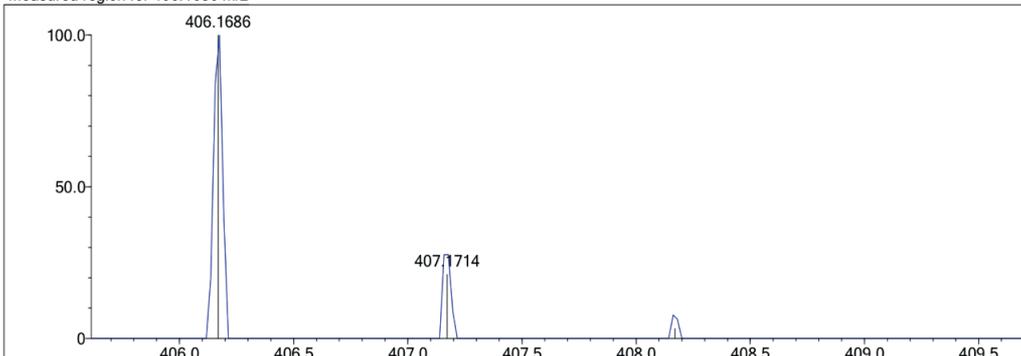
C22 H23 N5 O S [M+H]+ : Predicted region for 406.1696 m/z
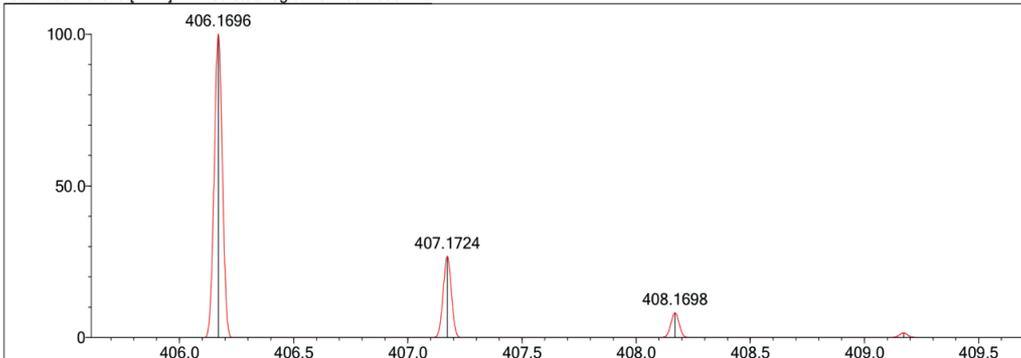
Rank	Score	Formula (M)	Ion	Meas. m/z	Pred. m/z	Df. (mDa)	Df. (ppm)	Iso	DBE
1	81.39	C22 H23 N5 O S	[M+H]+	406.1686	406.1696	-1.0	-2.46	84.48	14.0

Figure S3. Compound **3a** HRMS report
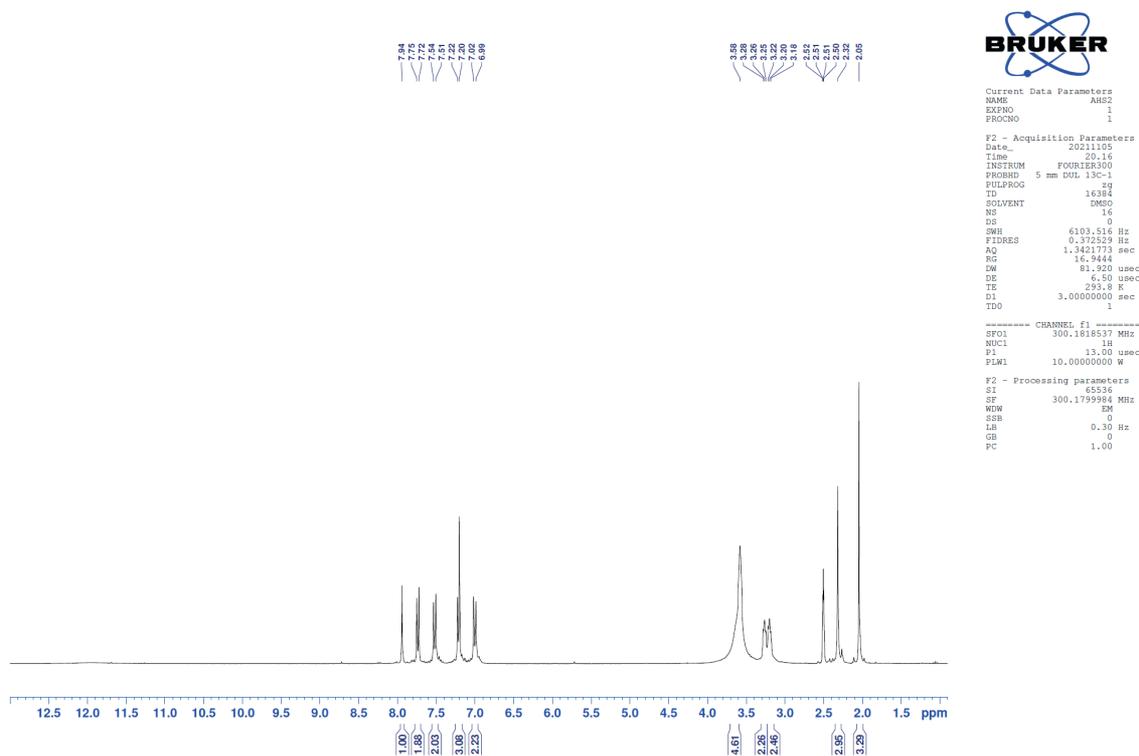
Figure S4. Compound **3b** ^{1}H-NMR spectrum
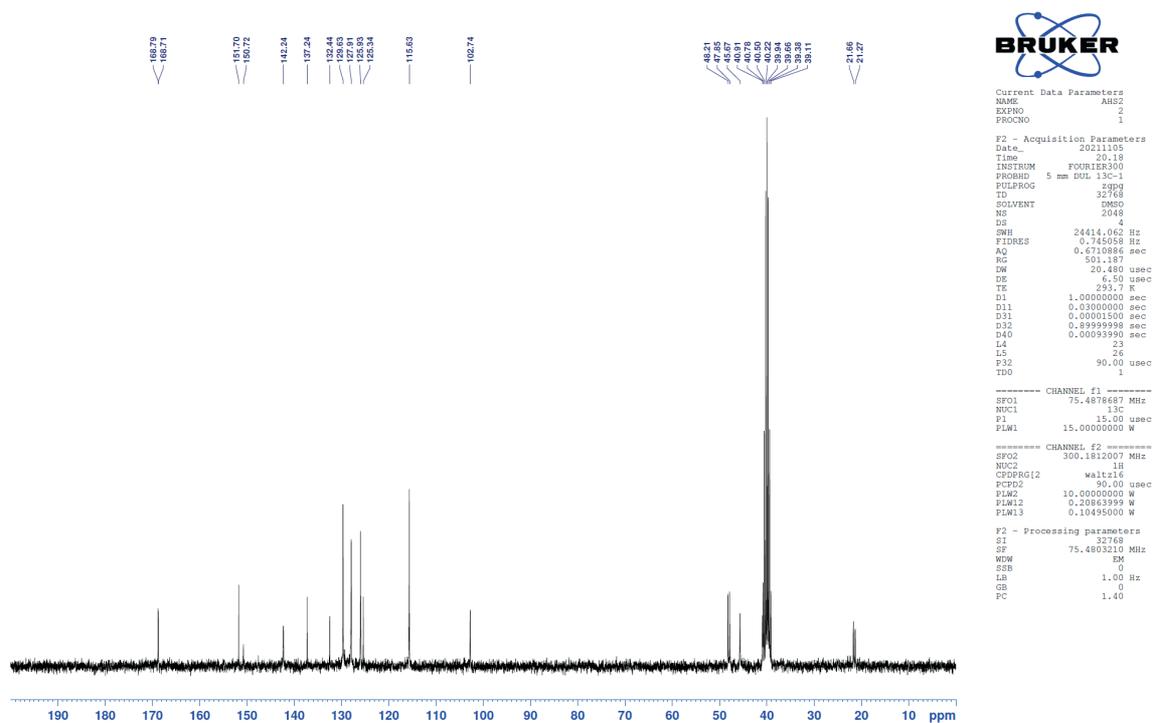
Figure S5. Compound **3b** ^{13}C-NMR spectrum

Formula Predictor Report - AHS-2_112.lcd

Data File: C:\LabSolutions\Data\Analiz\derya\AHS-2_112.lcd

Elmt	Val.	Min	Max	Elmt	Val.	Min	Max	Elmt	Val.	Min	Max	Elmt	Val.	Min	Max	Use Adduct
H	1	6	46	O	2	0	3	S	2	0	2	Ru	2	0	0	H
C	4	5	36	F	1	0	0	Cl	1	0	0	Pd	2	0	0	
N	3	0	6	P	3	0	0	Br	1	0	0	I	3	0	0	

|		
Error Margin (ppm): 5	DBE Range: 0.0 - 30.0	Electron Ions: both
HC Ratio: unlimited	Apply N Rule: yes	Use MSn Info: yes
Max Isotopes: 3	Isotope RI (%): 1.00	Isotope Res: 9000
MSn Iso RI (%): 10.00	MSn Logic Mode: AND	Max Results: 50

Event#: 1 MS(E+) Ret. Time : 5.347 Scan# : 803
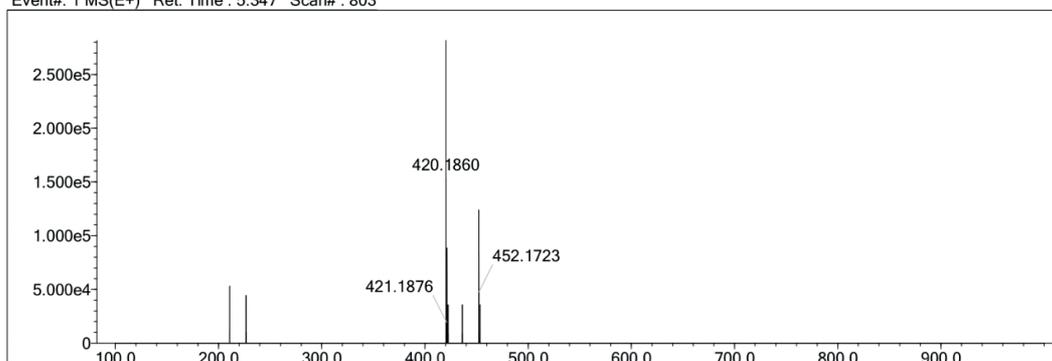
Measured region for 420.1860 m/z
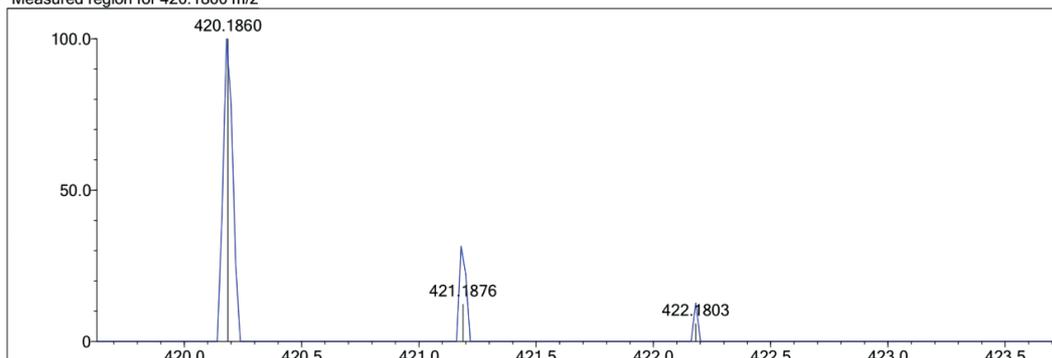
C23 H25 N5 O S [M+H]+ : Predicted region for 420.1853 m/z
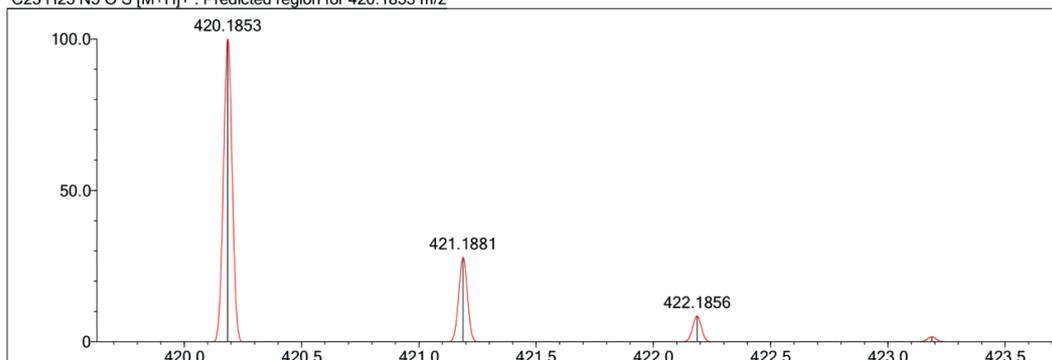
Rank	Score	Formula (M)	Ion	Meas. m/z	Pred. m/z	Df. (mDa)	Df. (ppm)	Iso	DBE
1	68.79	C23 H25 N5 O S	[M+H]+	420.1860	420.1853	0.7	1.67	69.96	14.0

Figure S6. Compound **3b** HRMS report
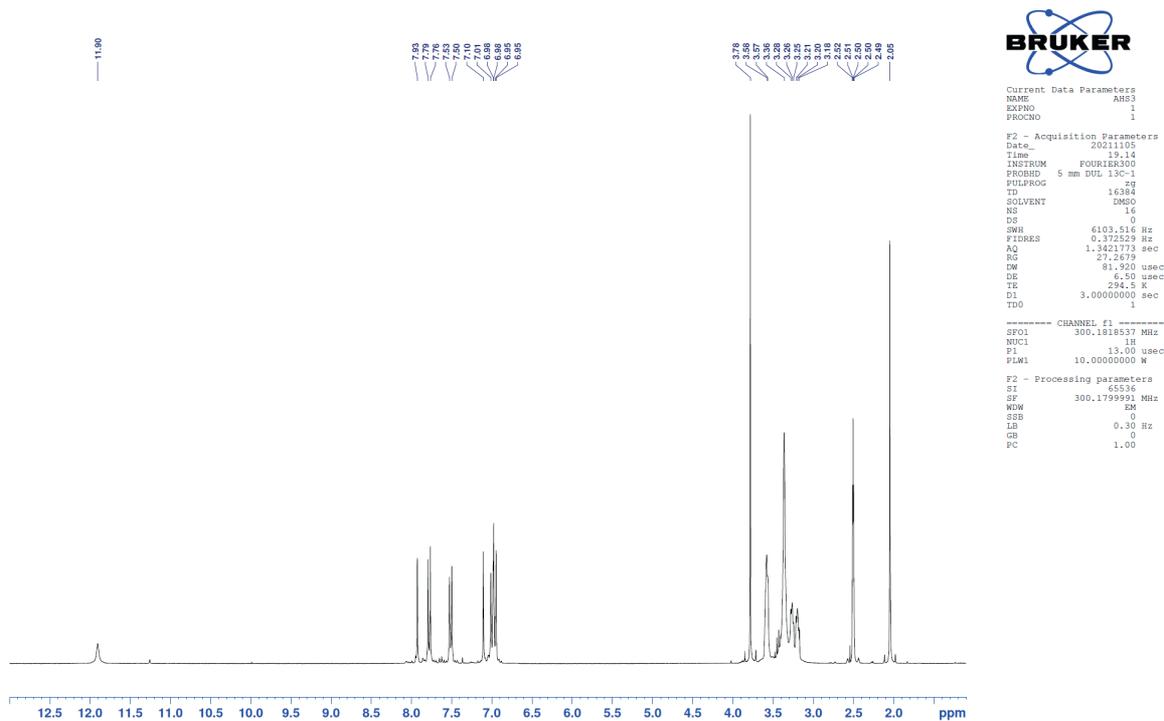
Figure S7. Compound **3c** ^{1}H-NMR spectrum
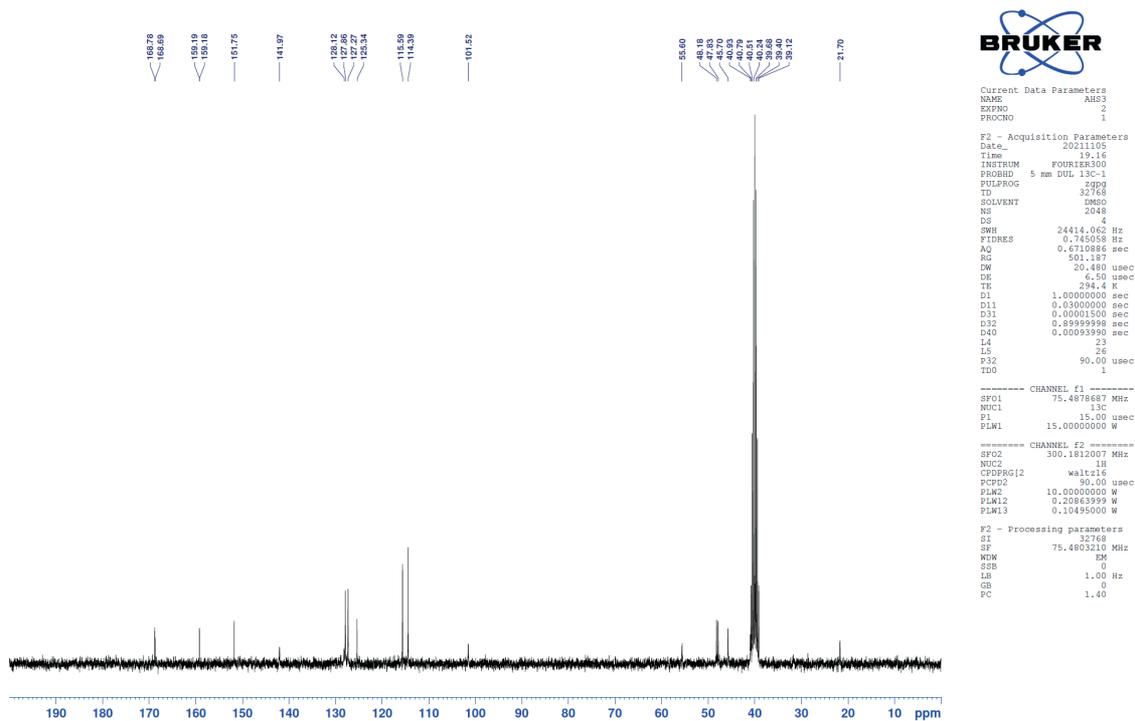

Figure S8. Compound **3c** ^{13}C-NMR spectrum

Formula Predictor Report - AHS-3_104.lcd   Page 1 of 1

Data File: C:\LabSolutions\Data\Analiz\derya\AHS-3_104.lcd

Elmt	Val.	Min	Max	Elmt	Val.	Min	Max	Elmt	Val.	Min	Max	Elmt	Val.	Min	Max	Use Adduct
H	1	6	46	O	2	0	3	S	2	0	2	Ru	2	0	0	H
C	4	5	36	F	1	0	0	Cl	1	0	0	Pd	2	0	0	
N	3	0	6	P	3	0	0	Br	1	0	0	I	3	0	0	

Error Margin (ppm): 5   DBE Range: 0.0 - 30.0   Electron Ions: both
        HC Ratio: unlimited   Apply N Rule: yes   Use MSn Info: yes
    Max Isotopes: 3   Isotope RI (%): 1.00   Isotope Res: 9000
  MSn Iso RI (%): 10.00   MSn Logic Mode: AND   Max Results: 50

Event#: 1 MS(E+) Ret. Time : 4.387 Scan# : 659
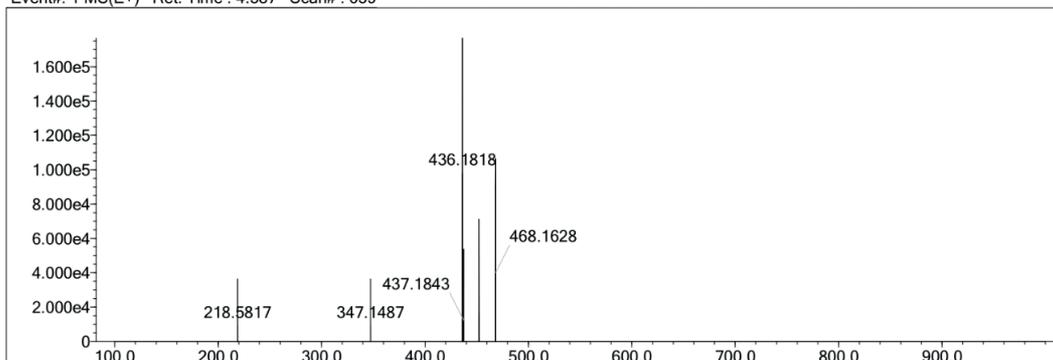
Measured region for 436.1818 m/z
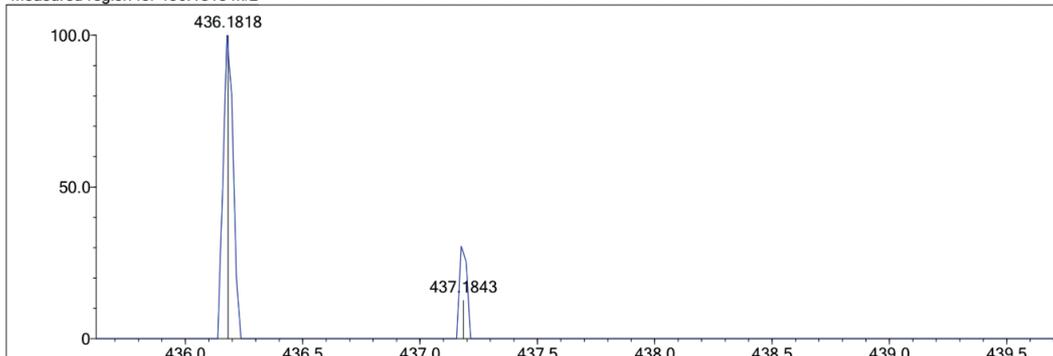
C23 H25 N5 O2 S [M+H]+ : Predicted region for 436.1802 m/z
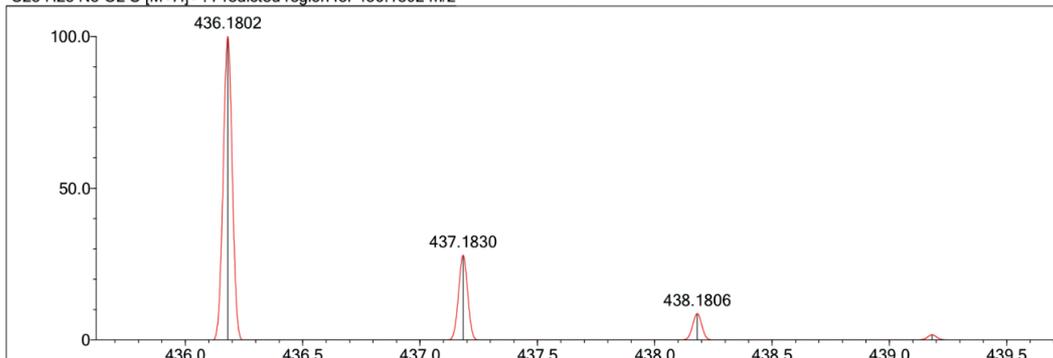
Rank	Score	Formula (M)	Ion	Meas. m/z	Pred. m/z	Df. (mDa)	Df. (ppm)	Iso	DBE
2	0.00	C23 H25 N5 O2 S	[M+H]+	436.1818	436.1802	1.6	3.67	0.00	14.0

Figure S9. Compound **3c** HRMS report
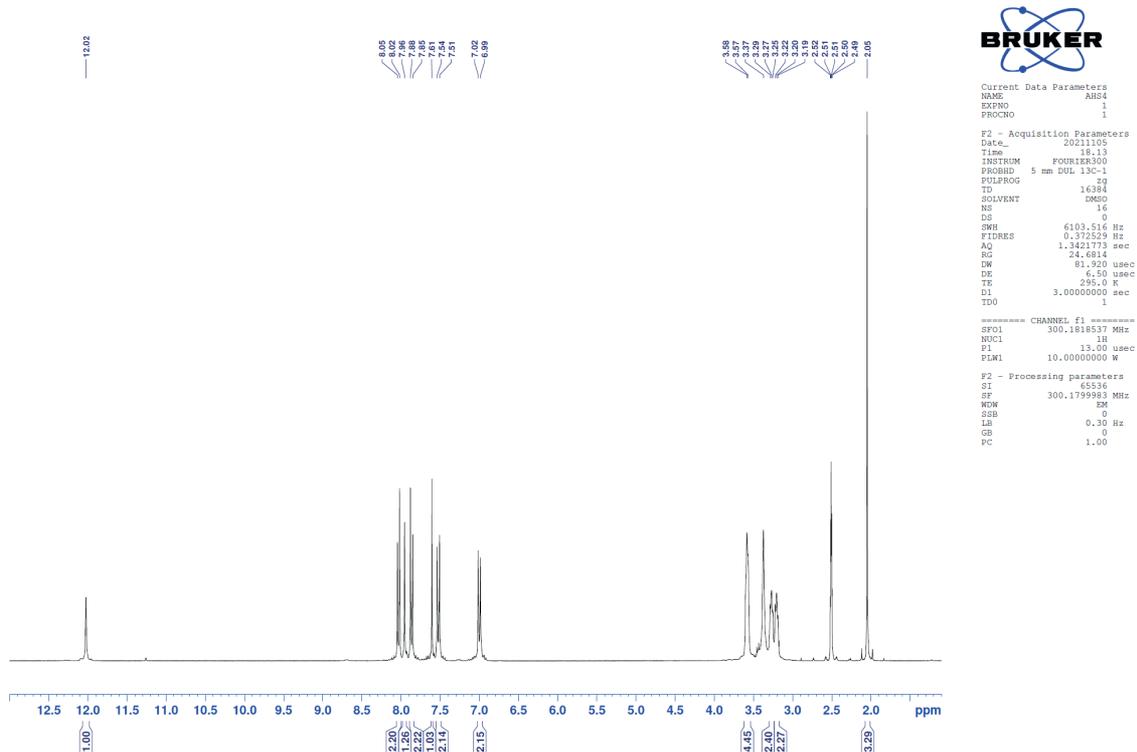
Figure S10. Compound **3d** ¹H-NMR spectrum
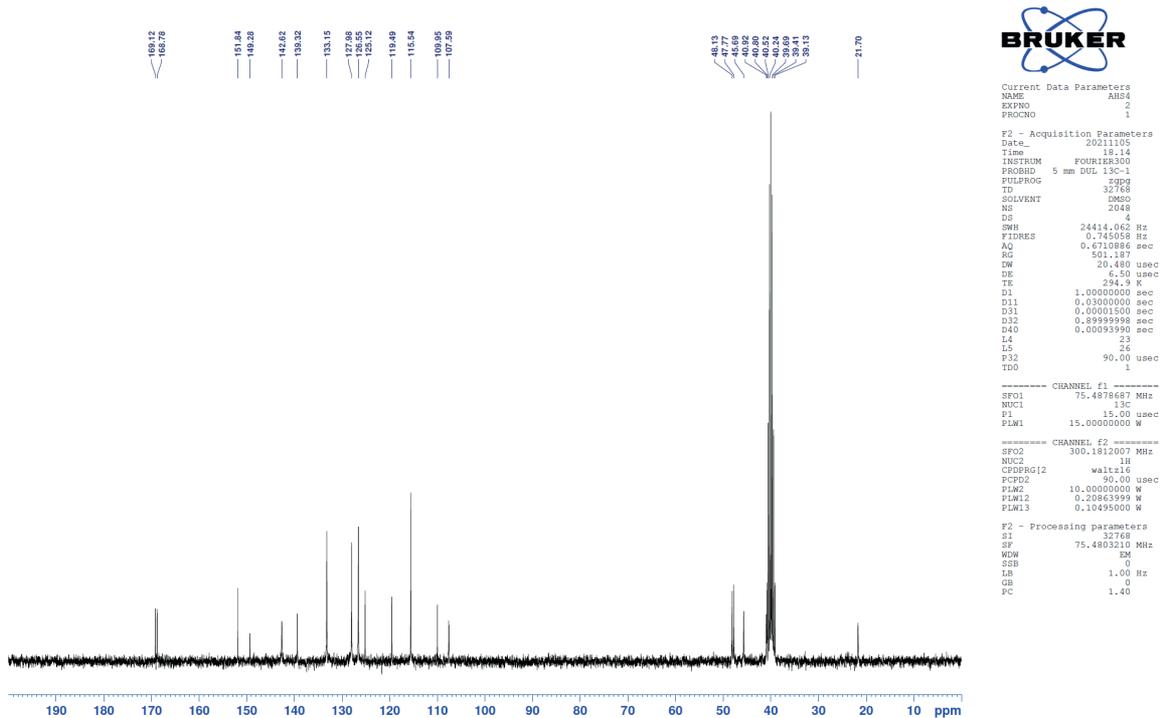
Figure S11. Compound **3d** ¹³C-NMR spectrum

Formula Predictor Report - AHS-4_114.lcd   Page 1 of 1

Data File: C:\LabSolutions\Data\Analiz\derya\AHS-4_114.lcd

Elmt	Val.	Min	Max	Elmt	Val.	Min	Max	Elmt	Val.	Min	Max	Elmt	Val.	Min	Max	Use Adduct
H	1	6	46	O	2	0	3	S	2	0	2	Ru	2	0	0	H
C	4	5	36	F	1	0	0	Cl	1	0	0	Pd	2	0	0	
N	3	0	6	P	3	0	0	Br	1	0	0	I	3	0	0	

Error Margin (ppm): 5   DBE Range: 0.0 - 30.0   Electron Ions: both
HC Ratio: unlimited   Apply N Rule: yes   Use MSn Info: yes
Max Isotopes: 3   Isotope RI (%): 1.00   Isotope Res: 9000
MSn Iso RI (%): 10.00   MSn Logic Mode: AND   Max Results: 50

Event#: 1 MS(E+) Ret. Time : 4.227 Scan# : 635
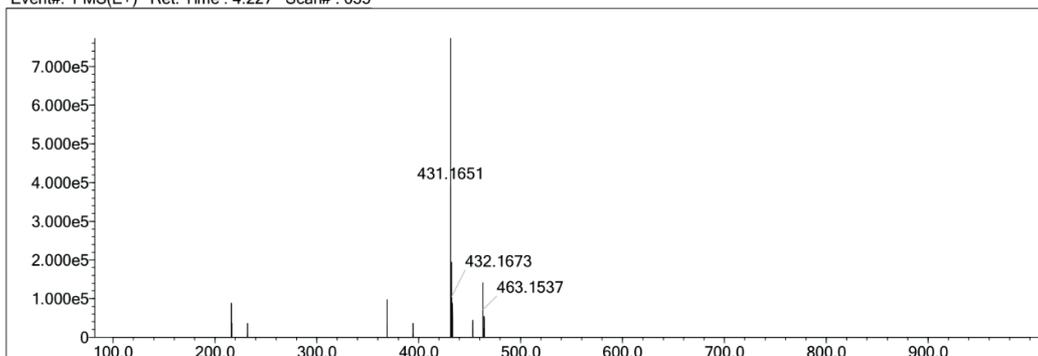
Measured region for 431.1651 m/z
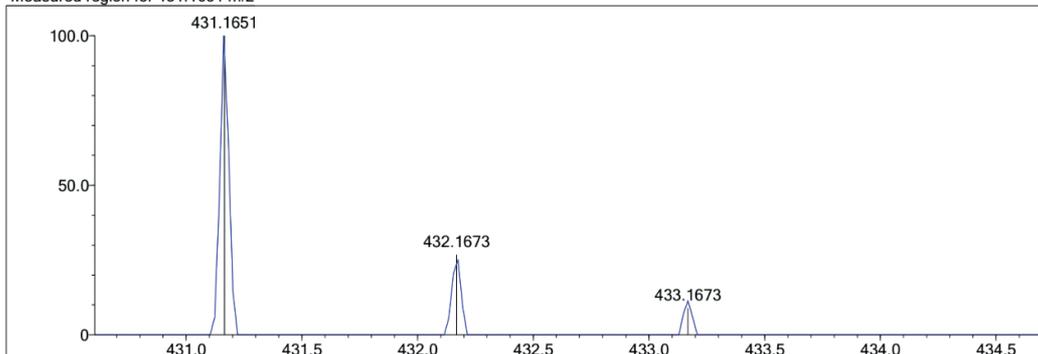
C23 H22 N6 O S [M+H]+ : Predicted region for 431.1649 m/z
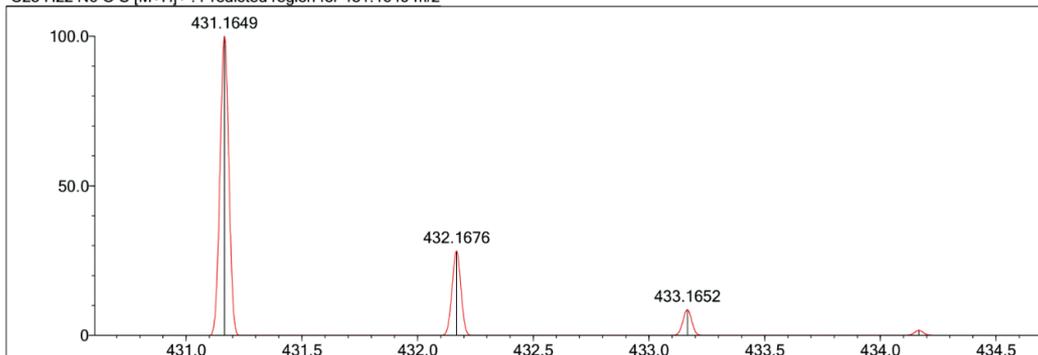
Rank	Score	Formula (M)	Ion	Meas. m/z	Pred. m/z	Df. (mDa)	Df. (ppm)	Iso	DBE
1	77.87	C23 H22 N6 O S	[M+H]+	431.1651	431.1649	0.2	0.46	77.87	16.0

**Figure S12.** Compound **3d** HRMS report
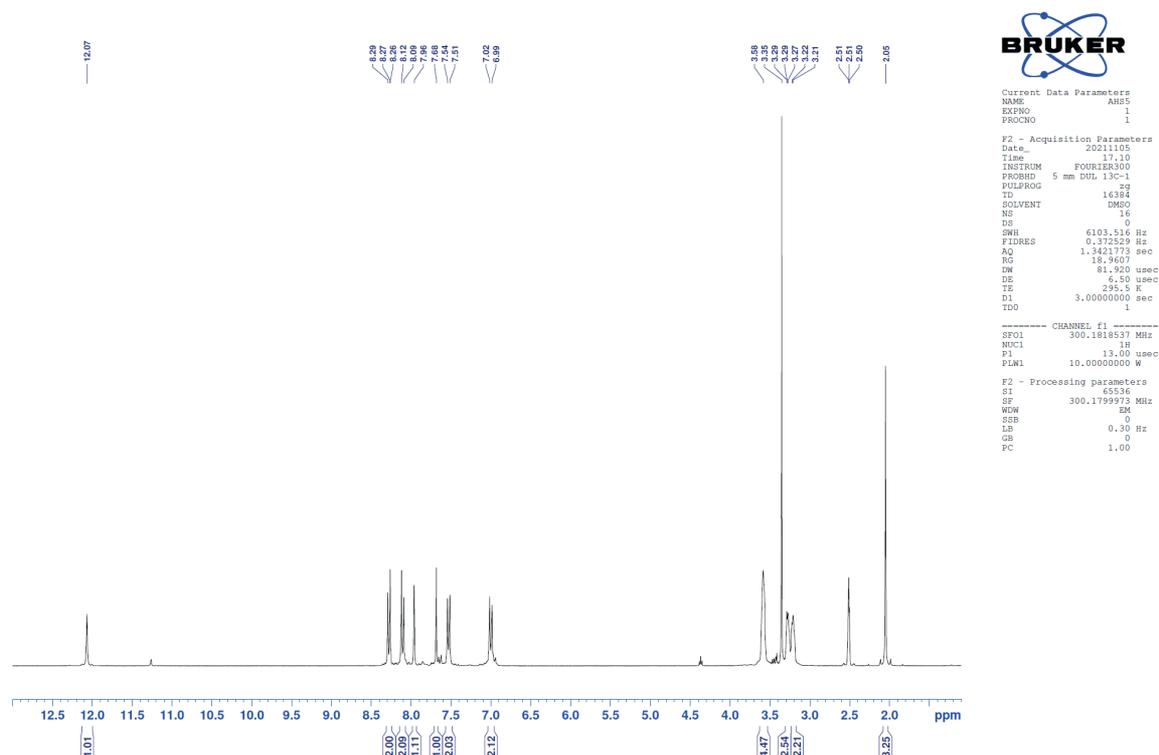
Figure S13. Compound **3e** ¹H-NMR spectrum
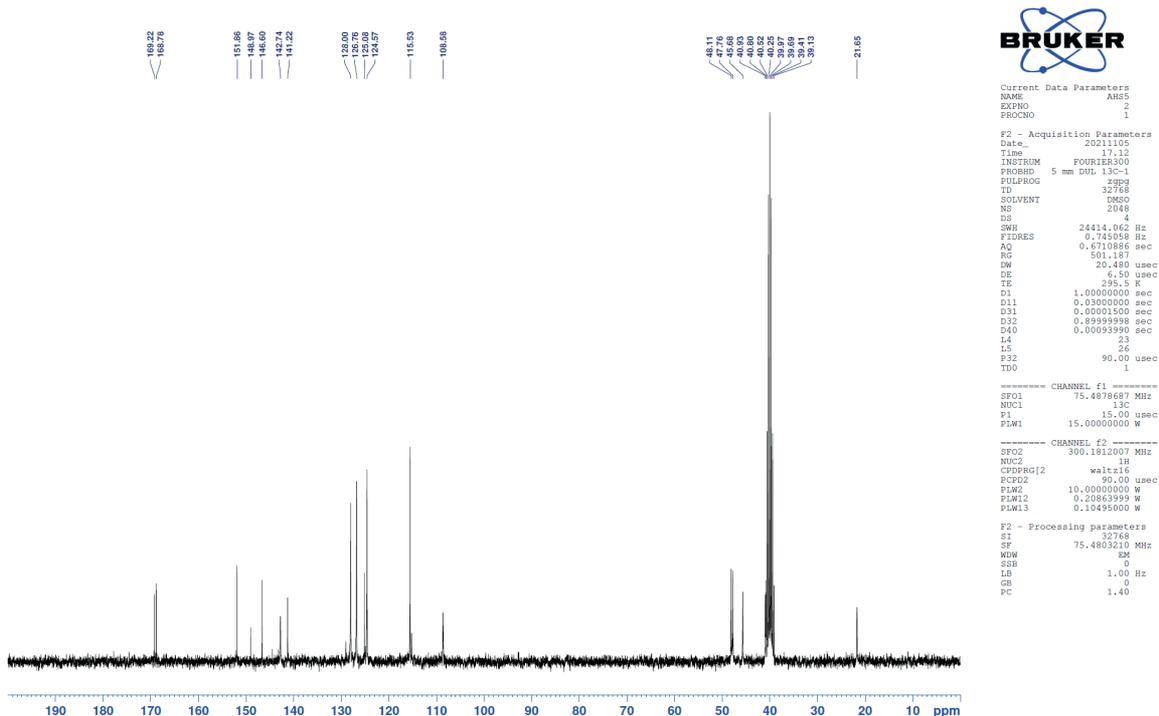
**Figure S14.** Compound **3e** ¹³C-NMR spectrum

Formula Predictor Report - AHS-5_105.lcd

Data File: C:\LabSolutions\Data\Analiz\derya\AHS-5_105.lcd

| Elmt	Val.	Min	Max	Elmt	Val.	Min	Max	Elmt	Val.	Min	Max	Elmt	Val.	Min	Max	Use Adduct
H	1	6	46	O	2	0	3	S	2	0	2	Ru	2	0	0	H
C	4	5	36	F	1	0	0	Cl	1	0	0	Pd	2	0	0	
N	3	0	6	P	3	0	0	Br	1	0	0	I	3	0	0	

Error Margin (ppm): 5
HC Ratio: unlimited
Max Isotopes: 3
MSn Iso RI (%): 10.00

DBE Range: 0.0 - 30.0
Apply N Rule: yes
Isotope RI (%): 1.00
MSn Logic Mode: AND

Electron Ions: both
Use MSn Info: yes
Isotope Res: 9000
Max Results: 50

Event#: 1 MS(E+)   Ret. Time : 4.760   Scan# : 715
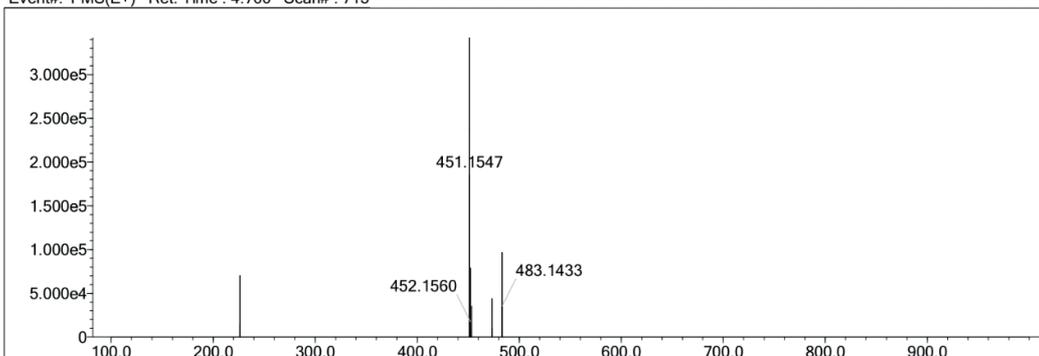
Measured region for 451.1547 m/z
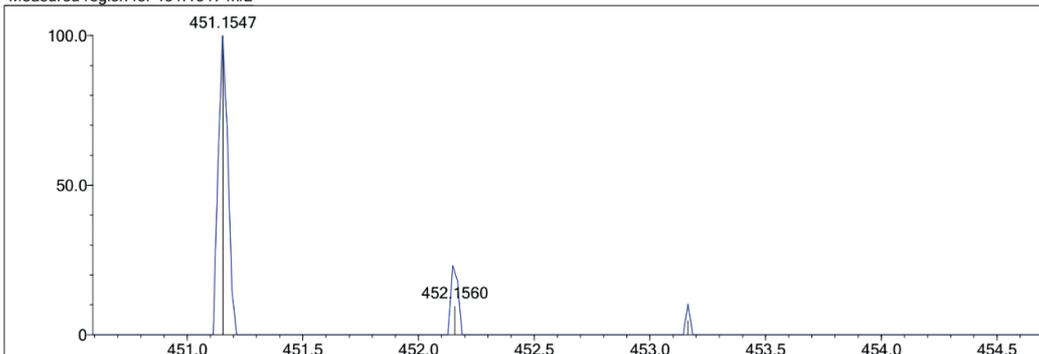
C22 H22 N6 O3 S [M+H]+ : Predicted region for 451.1547 m/z
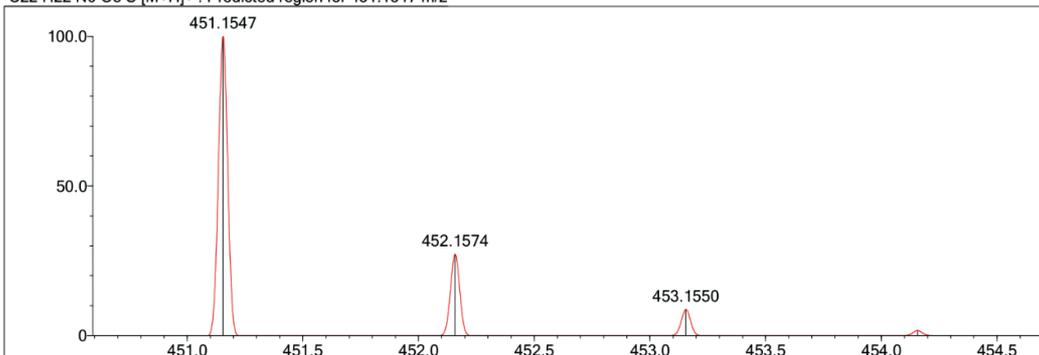
Rank	Score	Formula (M)	Ion	Meas. m/z	Pred. m/z	Df. (mDa)	Df. (ppm)	Iso	DBE
2	56.75	C22 H22 N6 O3 S	[M+H]+	451.1547	451.1547	0.0	0.00	56.75	15.0

Figure S15. Compound **3e** HRMS report
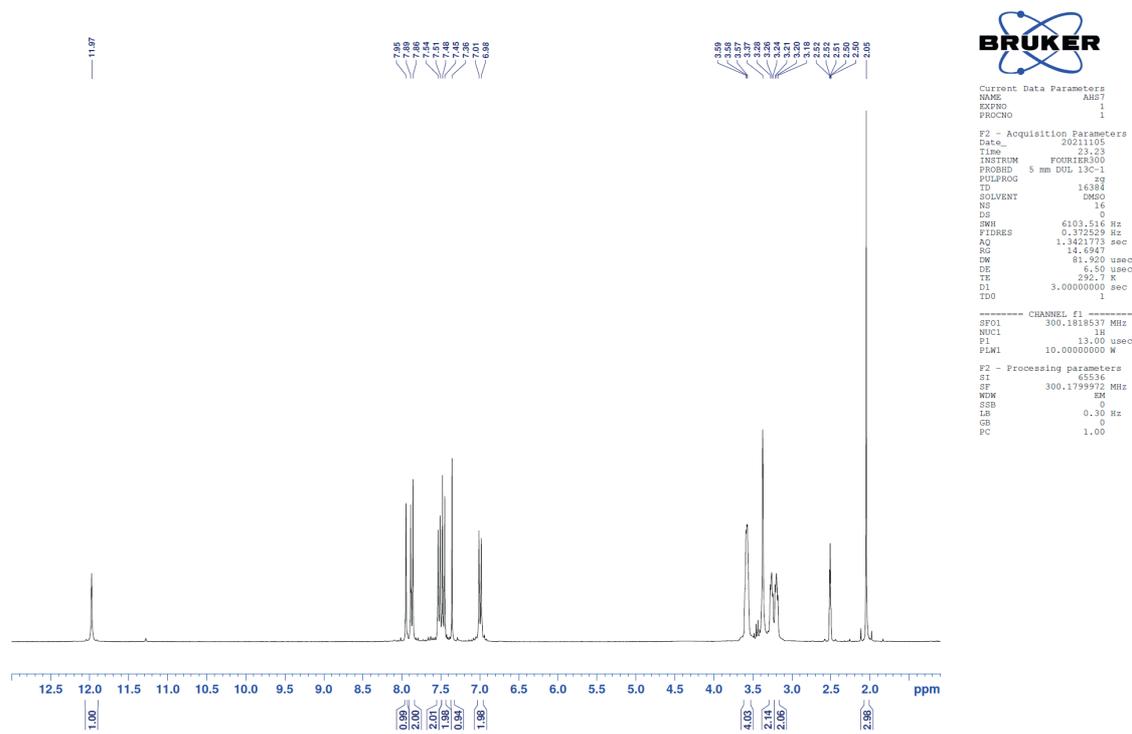
Figure S16. Compound **3f** [^1]H-NMR spectrum
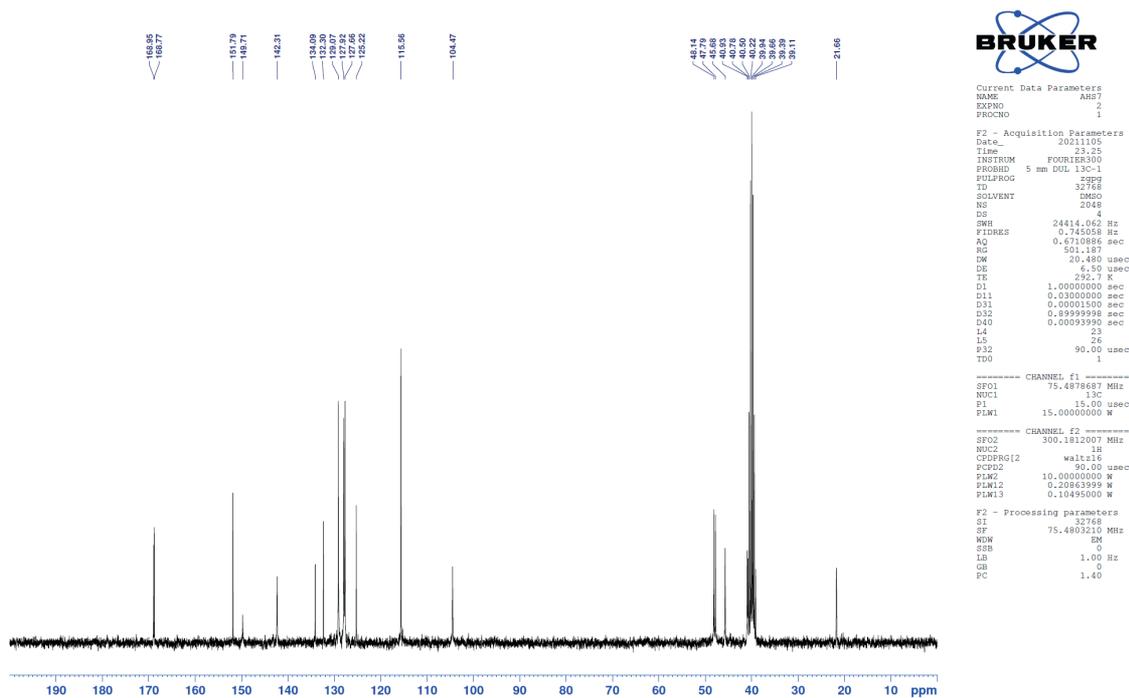
Figure S17. Compound **3f** [^13]C-NMR spectrum

Formula Predictor Report - AHS-7_116.lcd

Data File: C:\LabSolutions\Data\Analiz\derya\AHS-7_116.lcd

Elmt	Val.	Min	Max	Elmt	Val.	Min	Max	Elmt	Val.	Min	Max	Elmt	Val.	Min	Max	Use Adduct
H	1	6	46	O	2	0	3	S	2	0	2	Ru	2	0	0	H
C	4	5	36	F	1	0	0	Cl	1	1	1	Pd	2	0	0	
N	3	0	6	P	3	0	0	Br	1	0	0	I	3	0	0	

Error Margin (ppm): 5
HC Ratio: unlimited
Max Isotopes: 3
MSn Iso RI (%): 10.00

DBE Range: 0.0 - 30.0
Apply N Rule: yes
Isotope RI (%): 1.00
MSn Logic Mode: AND

Electron Ions: both
Use MSn Info: yes
Isotope Res: 9000
Max Results: 50

Event#: 1 MS(E+) Ret. Time : 6.013 Scan# : 903
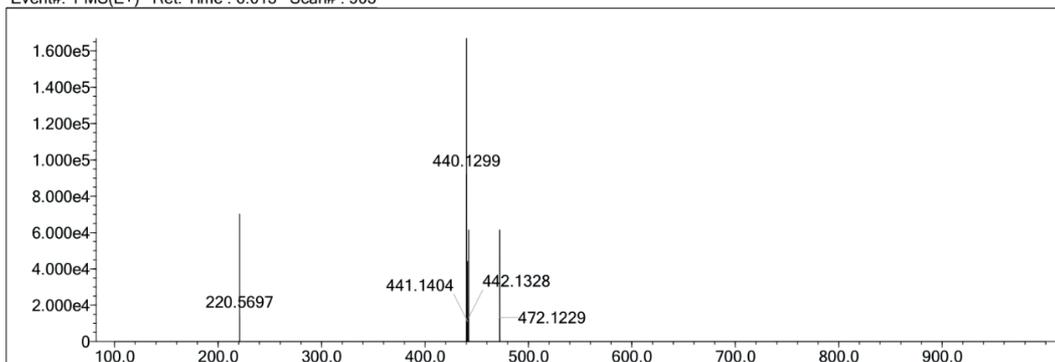
Measured region for 440.1299 m/z
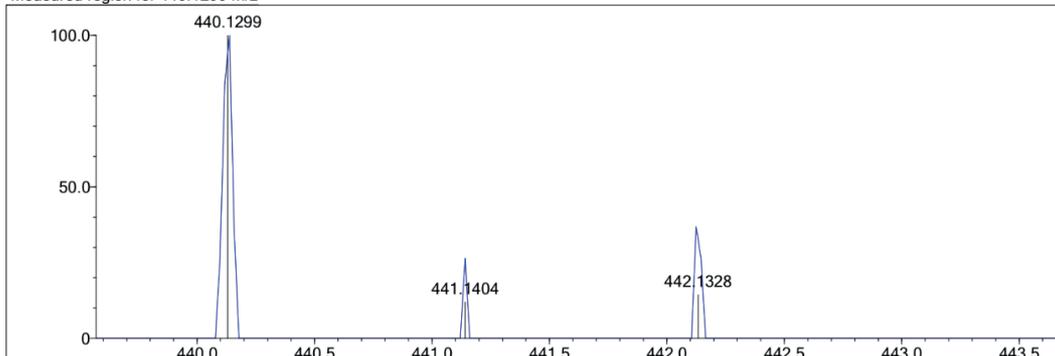
C22 H22 N5 O S Cl [M+H]+ : Predicted region for 440.1306 m/z
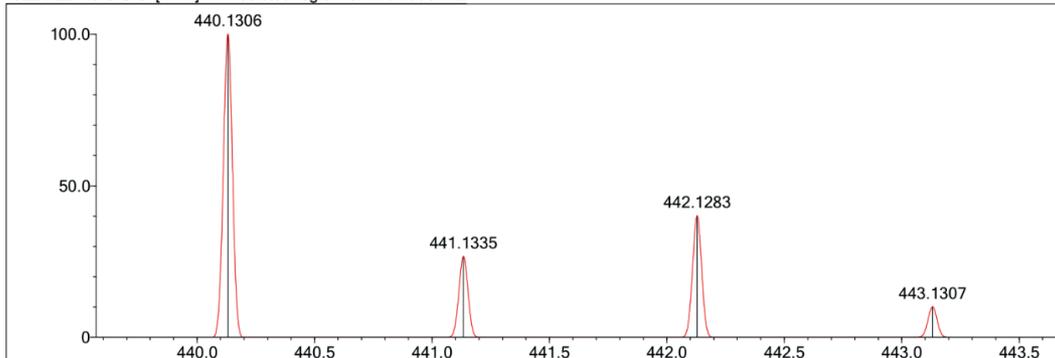
Rank	Score	Formula (M)	Ion	Meas. m/z	Pred. m/z	Df. (mDa)	Df. (ppm)	Iso	DBE
1	50.93	C22 H22 N5 O S Cl	[M+H]+	440.1299	440.1306	-0.7	-1.59	51.70	14.0

Figure S18. Compound **3f** HRMS report
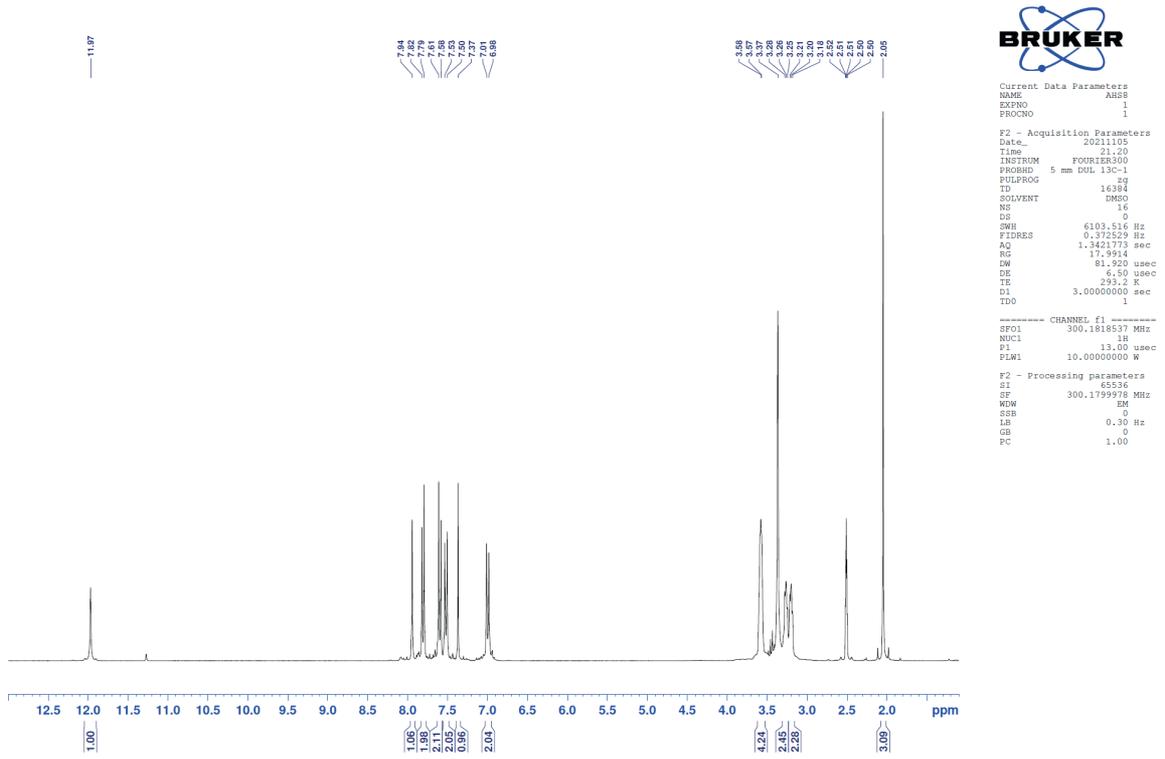
**Figure S19.** Compound **3g** ^{1}H-NMR spectrum
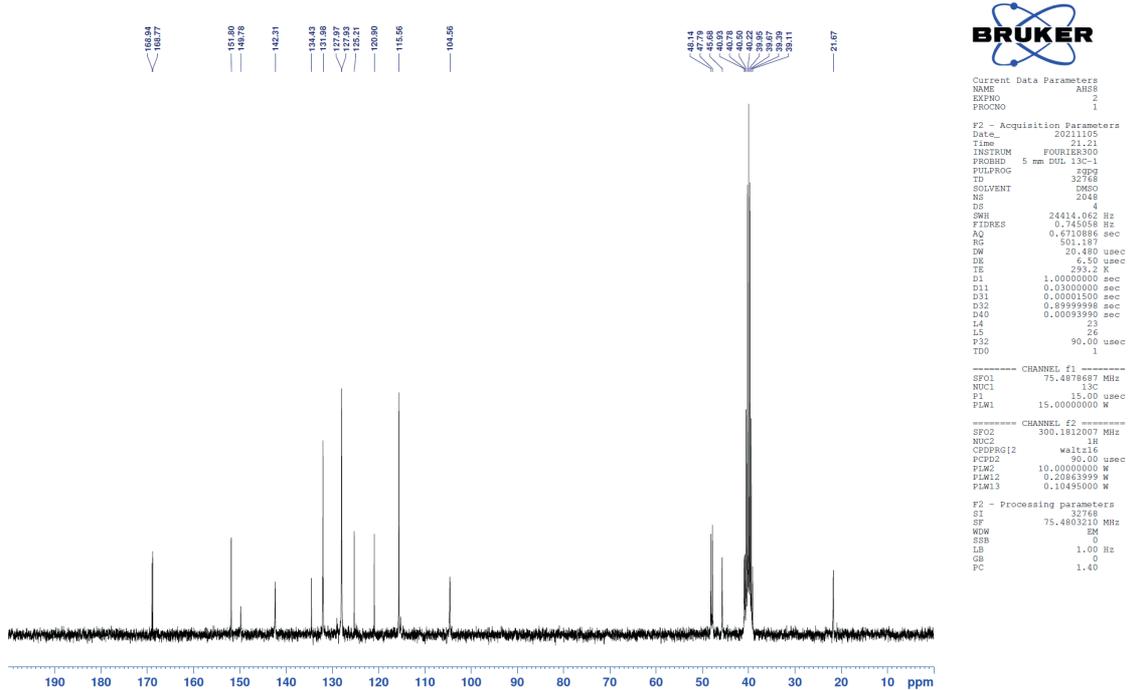

Figure S20. Compound **3g** ^{13}C-NMR spectrum

Formula Predictor Report - AHS-8_455.lcd   Page 1 of 1

Data File: C:\LabSolutions\Data\Analiz\derya\AHS-8_455.lcd

Elmt	Val.	Min	Max	Elmt	Val.	Min	Max	Elmt	Val.	Min	Max	Elmt	Val.	Min	Max	Use Adduct
H	1	6	46	O	2	0	3	S	2	1	1	Ru	2	0	0	H
C	4	5	36	F	1	0	0	Cl	1	0	0	Pd	2	0	0	Na
N	3	0	6	P	3	0	0	Br	1	1	1	I	3	0	0	

Error Margin (ppm): 5   DBE Range: 0.0 - 30.0   Electron Ions: both
        HC Ratio: unlimited   Apply N Rule: yes   Use MSn Info: yes
      Max Isotopes: 3   Isotope RI (%): 1.00   Isotope Res: 9000
   MSn Iso RI (%): 10.00   MSn Logic Mode: AND   Max Results: 50

Event#: 1 MS(E+) Ret. Time : 9.307 Scan# : 1397
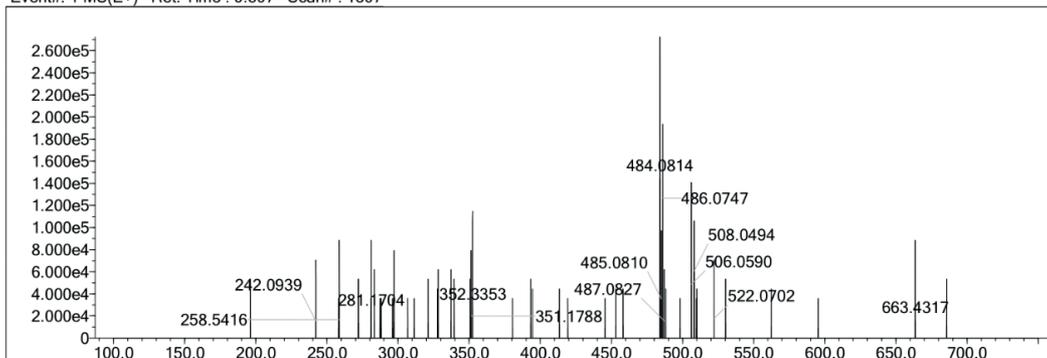
Measured region for 484.0814 m/z
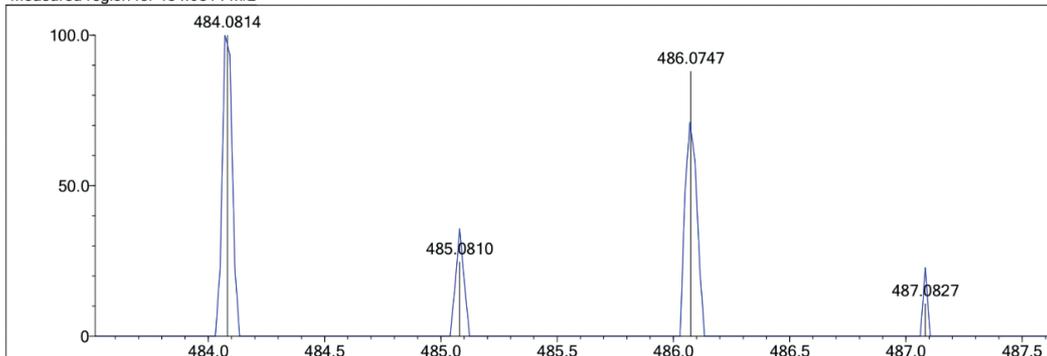
C22 H22 N5 O S Br [M+H]+ : Predicted region for 484.0801 m/z
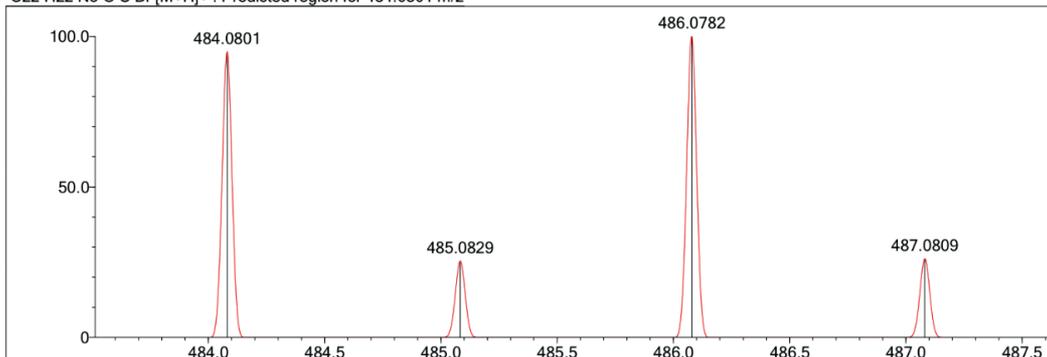
Rank	Score	Formula (M)	Ion	Meas. m/z	Pred. m/z	Df. (mDa)	Df. (ppm)	Iso	DBE
1	50.89	C22 H22 N5 O S Br	[M+H]+	484.0814	484.0801	1.3	2.69	53.13	14.0

Figure S21. Compound **3g** HRMS report